Pelletization and Thermo-Catalytic Reforming of Municipal Solid Waste

by

Benjamin Mauricio Martinez Castellanos

A thesis submitted in partial fulfillment of the requirements for the degree of

Master of Science

in

Engineering Management

Department of Mechanical Engineering
University of Alberta

Abstract

Meeting the objectives of the Paris Agreement requires society to reduce greenhouse gas (GHG) emissions levels in every sector. Waste management has a key role in achieving these objectives and is fundamental for sustainable growth. Some municipal solid waste (MSW) streams have the potential for waste-to-energy conversion, thereby increasing the waste diversion rate. Thermo-catalytic reforming (TCR) is a conversion method based on pyrolysis that allows the conversion of an organic feedstock into valuable products like bio-oil, biochar, and syngas. TCR requires a homogeneous feedstock that can be produced through pelletization. There is very little information available on utilization of different components of MSW streams for production of liquid fuel production using TCR. This research work is an effort to address this gap.

The first part of this study focuses on the size reduction and pelletization of fractions of the municipal solid waste, that is, digestate, source-separated organics (SSO), and refuse-derived fuel (RDF). The effect of particle size and moisture content in the grinding and pelletization was assessed at a laboratory scale. While the digestate could not be pelletized, SSO and RDF pellets were successfully produced. The highest pellet durability values were 98.2 % for RDF and 97.4 % for SSO. The specific energy consumption for grinding and pelletization was as low as 2281.15 KJ/kg for RDF and 489.49 KJ/kg for SSO. The RDF pellets showed a high heating value (HHV) of 21.5 MJ/kg and an ash content of 9.8 %. Seasonal variation was observed in the SSO pellets, with a lower HHV (13.9 MJ/kg) and higher ash content (34.7 %) during the spring/summer seasons and a higher HHV (19.5 MJ/kg) and lower ash content (13.51 %) during the winter season.

In the second part of this study, a 2 kg/h lab scale TCR unit was used to investigate the thermo-catalytic reforming of SSO pellets. Two pyrolysis reactor temperatures (400 °C and 500 °C) and three post-reformer temperatures (500 °C, 600 °C, and 650 °C) were used to study the effects of process temperature on product yields and characteristics. At higher process temperatures of 500 °C in the reactor and 650 °C in the reformer, the highest energy conversion efficiency of 92.37 % was achieved. These conditions also yielded a higher syngas production of 42.79 % with an HHV of 19.13 MJ/kg. Higher temperatures resulted in lower bio-oil yields of 2.11 % but improved quality, that is, the viscosity, oxygen content, and total acid number were reduced. Lower process temperatures resulted in a maximum bio-oil yield of 6.20 % with an HHV of 37.2 MJ/kg. The effect of temperature on bio-oil characteristics was also examined. Biochar had an HHV of 9.25 to 10.24 MJ/kg and a yield between 41.17 % and 46.25 %. The information developed in this research can help in understanding the potential pathways of utilization of MSW for liquid and gaseous fuel production.

Preface

This thesis is an original research work conducted by me, Benjamin Mauricio Martinez Castellanos, at the University of Alberta under the supervision of Professor Amit Kumar.

The second chapter of this thesis, titled "The pelletization of three municipal solid waste streams: Digestate, source-separated organics and refuse-derived fuel," by Benjamin Mauricio Martinez, Omex Mohan, Vinoj Kurian, Neelanjan Bhattacharjee, and Amit Kumar, will be submitted to a peer-reviewed journal.

The third chapter of this thesis, titled "The thermo-catalytic reforming of the source-separated organics," by Benjamin Mauricio Martinez, Neelanjan Bhattacharjee, and Amit Kumar, will be submitted to a peer-reviewed journal.

I was responsible for all the experimental work, including data collection, analysis, and deliverables writing. Other authors helped in preparation of the material and the review of the manuscripts. Professor Amit Kumar was the supervisory author and played a key role in overall supervision, conceptualization, planning, analysis and validation of results and manuscript edits.

Dedicated to my parents, Benjamin and Lilia.

friend, Diego Carvajal; his advice and friendship have meant a lot to me, even more from the distance.

Table of Contents

List of Tables

List of Figures

List of Abbreviations

ACETA   Alberta Clean Energy Technology Accelerator

AD   Anaerobic Digestion

ADL   Acid detergent lignin

ADF   Acid detergent fiber

EWMC   Edmonton Waste Management Centre

GC   Gas chromatograph

GHG   Greenhouse gas

HHV   High heating value

IEA   International Energy Agency

MAH   Monocyclic aromatic hydrocarbons

MC   Moisture content

MS   Mass spectrometer

MSW   Municipal solid waste

NDF   Neutral detergent fiber

PAH   Polycyclic aromatic hydrocarbons

RDF   Refuse-derived fuels

RSW   Residential solid waste

SEC   Specific energy consumption

SSO   Source-separated organics

TAN   Total acid number

TCR   Thermo-catalytic reforming

THF   Tetrahydrofuran

Chapter 1: Introduction

1.1 Background

As the world expands economically and demographically, extended efforts in sustainable development are called for to manage more efficiently the consequences of this growth. In the coming years, critical world challenges include meeting the objective of the Paris Agreement [1], which requires countries to reduce greenhouse gas (GHG) emissions by implementing mitigation measures in all sectors. According to GAIA's 2022 report [2], about 3.3 % of global emissions are from the waste management sector. In 2019, 1.63 billion tonnes of CO_2-equivalent were generated by the waste sector [3]. These numbers are relevant because by 2050 the emissions from waste could go up to 2.6 billion tonnes of CO_2-equivalent.

In Canada, the waste sector generates 3 % of GHG emissions and 22 % of the total methane emissions [4]. From a life cycle perspective, the waste sector may also be responsible for indirect GHG emissions from other sectors not directly associated with waste such as transportation, forestry, energy, and industrial processes. Waste prevention and diversion are the most effective ways to reduce GHG emissions. However, waste management practices need to be improved to reduce the environmental impact. At a national level, the diversion rate for organics is only 7 % [4] which means that most organic waste (93 %) is being sent to landfills or incinerators. This is concerning as organic waste can be composted, anaerobically digested, or pyrolyzed to produce valuable resources like fertilizer or biofuels. The diversion rate for recyclable materials is only 16 % [4], indicating another sizable improvement opportunity. Based on 2018 data [5], it is evident that the province of Alberta has the highest waste disposal rate per person, 958 kg/year. This figure is significantly higher than the national average of 694 kg/year. Furthermore, Alberta has a

diversion rate of 18.4 %, lower than the Canadian average of 27.6 %. These figures call for further enhancements of waste management practices in the province.

There are three basic waste diversion approaches: recycling, reusing, and composting [6]. In the reuse category, waste-to-energy conversion is one of the more sustainable, renewable, and environmentally friendly means of transforming waste streams into value-added sources of fuel that can replace conventional fossil fuels. Waste-to-energy technologies can be classified by the conversion method used, i.e., thermochemical, physicochemical, or biological. Thermochemical alternatives include incineration, liquefaction, torrefaction, pyrolysis, and gasification. Physicochemical conversion is mainly observed in transesterification, whereas biological conversion relies on fermentation, whose most known alternative is anaerobic digestion [7].

One of the thermochemical conversion techniques that enables the conversion of biomass feedstocks into valuable products is pyrolysis. This process involves heating the biomass in the absence of oxygen at high temperatures, which decomposes the organic matter. The result is the production of three main components: bio-oil, syngas, and biochar [7] [8]. Pyrolysis can be classified as slow, intermediate, and fast, depending on factors such as the process temperature, heating rates, and residence time [9]. The thermo-catalytic reforming (TCR) method developed by Fraunhofer UMSICHT [10] is an intermediate pyrolysis technology that incorporates a catalytic reforming process to improve the quality of the pyrolysis products [11].

In a municipality (e.g. City of Edmonton), typically, municipal solid waste (MSW) generated by households is sorted and collected in three streams: organics, ordinary waste, and recyclables. All of them are processed at a central facility. The waste treatment process generates various products, including source-separated organics (SSO), refuse-derived fuels (RDF), and digestate. All of them

can potentially be used as feedstock for waste-to-energy conversion approaches such as TCR. Previous research has been conducted on the application of TCR for processing biomass [12] and the organic fraction of municipal solid waste in Germany [13]. However, those studies were conducted outside Canada with feedstocks obtained through different treatment methods. Moreover, MSW characteristics have important differences among jurisdictions [14].

The TCR process requires a homogeneous feedstock to ensure a controlled mass flow rate and prevent obstructions in the moving components of the pyrolysis reactor. Considering the heterogeneous nature of the three streams, it is advantageous to process them to obtain homogeneous feedstocks that can be used in a consistent and controlled way. In this regard, pelletization presents a suitable option for meeting this requirement.

Several municipalities in the world have set goals of achieving net-zero by 2050 and have developed plans for managing their waste. As part of Edmonton's Zero Waste Framework defined by the local government, energy recovery from waste is one of the ways to reach the objectives established in the 25-year Waste Management Strategy [15]. This research aims at developing solutions for waste management for the different municipalities and help them in reaching their net-zero goals.

1.2 Research Objectives

This research aims to assess the suitability of SSO, RDF, and digestate for energy conversion, which includes the preprocessing, pelletization, and thermo-catalytic reforming of the feedstocks.

The specific objectives of this research are to:

- Assess the feasibility of pelletizing SSO, RDF, and digestate.

- Investigate the influence of particle size and moisture content on pelletization variables and pellet quality, identifying optimal variables for future scale-up work.

- Investigate the effect of reactor and reformer temperature on product yield and characteristics during the thermo-catalytic reforming of SSO pellets using a laboratory-scale TCR-2 unit.

- Characterize the physical properties, chemical composition, and energy content of the feedstocks, produced pellets, and TCR products.

1.3 Scope and limitations

1. This study was performed using the RDF, SSO, and digestate produced in Edmonton between September 2021 and August 2022. The feedstock characteristics and compositions are dependent on the households' waste disposal practices as well as the waste treatment process performed by the Edmonton Waste Management Centre.

2. The pelletization was studied by using feedstocks without the addition of binders or mixtures. Additional pelletization studies could be conducted with the addition of binders or mixtures of other biomass feedstocks.

3. Even though the pelletization was performed using two moisture content levels, the TCR experiments were carried out using only pellets with 10 % moisture content.

4. The produced RDF pellets were not used for TCR experiments because of a technical limitation of a maximum of 10 % plastics content in the TCR feedstock. This study could be extended to investigate the effect of adding RDF to any other suitable feedstock processed in the TCR unit.

5. Given that the digestate could not be pelletized, no TCR experiments were carried out using this feedstock.

6. The SSO pellets used for TCR were produced using the feedstock collected during the spring/summer seasons. This study could be extended to SSO pellets produced during the fall and winter seasons.

1.4 Thesis Outline

This thesis was written in a paper-based format and is composed of four chapters, described briefly below.

The first chapter includes the introduction, research objectives, scope and limitations, and thesis outline.

The second chapter, corresponding to the first paper, focuses on the pelletization of SSO, RDF, and digestate. The effects of grinding screen size and moisture content were investigated. An initial characterization of the feedstocks is presented, followed by a discussion of the effects of grinding screen size on the grinding process and a complete analysis of the pelletization variables and pellet quality for the different moisture contents and grinding sizes.

The third chapter describes the thermo-catalytic reforming of SSO pellets. The effects of reactor and reformer temperatures on the product's yield and characteristics were investigated. The energy content, physical properties, and chemical analysis of the TCR products are reported.

The last chapter provides the conclusions and future work recommendations.

Chapter 2: The pelletization of three municipal solid waste streams: Digestate, source-separated organics, and refuse-derived fuel generated in an urban municipality located in a colder region

2.1 Introduction

Residential solid waste (RSW) is one source of the municipal waste (MSW) generated in Edmonton, Alberta, Canada. It is collected through three waste streams grouped by the type of residue: organics and garden waste, ordinary residues, and recyclables. Each stream is processed separately at the Edmonton Waste Management Centre (EWMC) have location coordinates as 53°35'02.0"N 113°36'49.7"W. The organics and garden waste, also known as source-separated organics (SSO), is shredded and sent to the anaerobic digestion (AD) process. The ordinary residues pass through an initial screening, where they are sorted by size. Residues smaller than 3 inches are mechanically separated to obtain the organic fraction of RSW to be used as feedstock for the AD process; the by-product of AD is known as digestate. Residues between 5 and 9 inches are used in the refuse-derived fuel (RDF) production process. Stringfellow et al. [16] provide details of the operating principles of an RDF production plant that include the reception, treatment, and final materials separation.

Given the heterogeneous nature of the three streams mentioned above, it is required to process them to obtain homogeneous feedstocks that can be used in a consistent and controlled way. The densification process known as pelletization presents a suitable option for this purpose. Extensive research has been done on the pelletization of different biomass feedstocks [17] [18], including wood industry waste, agricultural and forest residues, and energy crops. Pradhan et al. [17]

identified the feedstock's moisture content, particle size, and composition as the pelletization parameters more frequently controlled.

Kratzeisen et al. [19] studied the suitability of digestate as a solid fuel through the combustion of two different high-maize silage pelletized digestates (50 % and 81 % maize feedstock). However, the authors did not explore the densification process in detail. Czekała et al. [20] proved that the digestate produced from the AD of manure, slurry, corn silage, and sugar beet pulp can be profitably densified in the form of pellets and briquettes, and Cathcart et al. [21] conducted a techno-economic analysis of digestate pellet production at existing AD plants. However, in both cases, very little emphasis was put on the digestate pelletization variables.

Several studies describe the composition of MSW [16] [14] [22]. Chavando et al. [14] illustrate how MSW characteristics vary with income level and how the jurisdiction and income level affect the composition of RDF; for instance, the waste generated by societies with higher income levels have more paper and cardboard and less food and green waste.

Rezaei et al. [23] studied the effects of particle size and moisture on the pelletization of a lab-prepared RDF feedstock with a pre-defined composition and found that lower particle sizes require more energy and generate a less durable pellet; the lowest pelletization energy was achieved with 20 % moisture content. García et al. [24] studied the co-pelletization of pine sawdust and RDF of a controlled composition and different mixing proportions, finding it feasible to pelletize mixes with both high and low RDF concentrations. Jewiarz et al. [25] studied in detail the mechanical variables involved in the pelletization of RDF generated in Krakow, Poland to redesign the dies for improved pellet quality. In their study, temperature played a significant role in the quality of the pellets; 120 °C was the most suitable pelletization temperature.

Earlier research has been conducted on the densification of food scraps. There is a trend towards applying a hydrothermal carbonization process to the food scraps, then using the generated hydrochar as the feedstock for pelletization. Moreira et al. [26] investigated the pelletization of the hydrochar obtained from food waste generated at restaurants along with the effect of adding ash and spent coffee grounds. Sharma et al. [27] studied the pelletization of the hydrochar produced from a mix of food waste generated at a hotel and yard waste from a university campus. Wang et al. [28] studied the pelletization of the biochar from a blend of food waste (obtained from a restaurant) and woody biomass along with the addition of molasses as a binder to pelletize the food waste hydrochar [29]. Chew et al. [30] worked on the pelletization of food waste compost and the effect of the addition of dairy powder in the pelletization process. Most of these studies used waste generated in a controlled environment such as hotels and restaurants; no research has been conducted on the organic fraction of MSW as an unprocessed material.

The literature review did not find any studies of the pelletization of digestate, RDF, or SSO produced from MSW in North America. Moreover, given that factors like kitchen household practices, municipal regulations, waste management systems, and seasonal effects decide the final composition of waste streams, it was identified that there is a need to study the pelletization of the different waste streams as they are delivered by municipal treatment facilities. This research focuses on the densification processes adapted for such real-life characteristics and compositions as well as the pelletization of three different waste streams – SSO, RDF, and digestate – generated in Edmonton, Alberta. The effect of grinding, ground material particle size, and feedstock moisture in the pelletization process was investigated and the suitability of each waste stream for further use as the feedstock for a waste-to-energy conversion approach was assessed.

2.2 Materials and Methods

2.2.1   Materials

Figure 1 shows the material process involving feedstock collection, moisture removal through dryings, followed by grinding and pelletization. The materials for the experimental work were provided by the EWMC. The dried, fermented, 28-day old samples (known as digestate) were procured from the high solids anaerobic batch digester [31] located in the Anaerobic Digestion Facility of the EWMC. The digestate consists of large chunks of organics, wood pieces from garden waste, and multiple non-organic materials that remain the same after the anaerobic digestion (AD) process, such as plastics and glass. Upon receipt, the samples were dried in a hot air oven maintained at 106 °C for 24 hours.

The SSO samples were taken from the pile of shredded organics ready to be fed into the anaerobic digestor. The material was mainly composed of organics (food scraps) with a minor presence of non-organic elements; once received, the SSO was also oven-dried at 106 °C for 24 hours. The major visible non-organic materials, such as plastics, paper, and cardboard, were manually removed to minimize contamination in the samples. Upon receipt, both the SSO and digestate were kept in a cold room to slow the degradation process. The dried materials were kept in closed containers at room temperature to avoid further degradation.
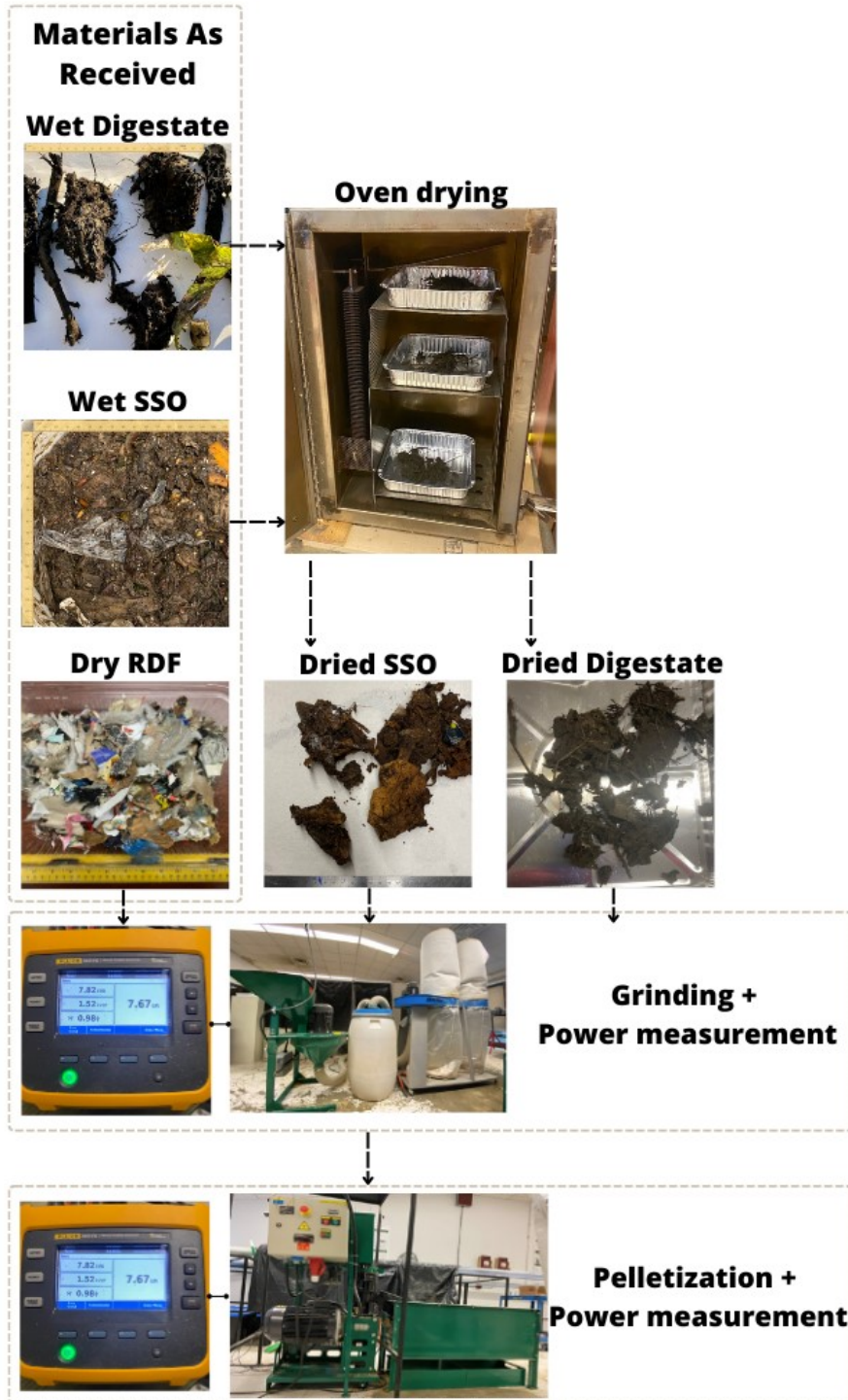
Figure 1: Process diagram.

Semi-dry RDF was provided by the EWMC's Integrated Processing and Transfer Facility. **Table 1** shows the estimated composition of the RDF based on measurements conducted by the production plant over an 18-month period; the reported values were based on the average of five batches of samples.

Table 1: RDF Composition.

Material	Average (%)	Std Dev (%)_
Paper	33.66	10.57
Film Plastic	27.04	2.50
Rigid Plastic	14.89	5.31
Fabric	9.45	3.38
Metal	1.17	1.30
Glass	0.05	0.05
Ceramic	0.0	0.01
Food Waste	0.60	0.53
Wood/Yard Waste	9.01	8.93
Other	2.99	2.58
Fines	1.14	3.32

The moisture content was measured at 106 °C for 24 hours to keep track of the moisture at all stages of the feedstock process. The stages included were as received, ground, conditioned before pelletization, and produced pellets.

A LECO 701 thermogravimetric analyzer was used, following ASTM D7582 [32], to determine the moisture, fixed carbon, volatiles, and ash content of the materials. Initially, the moisture content was calculated by keeping the sample at 106 °C until constant mass readings were received. The volatiles and fixed carbon contents were calculated by heating the samples to 900 °C and a holding time of 15 min with a heating rate of 40 °C/min in an oxygen-free atmosphere. The ash content was determined from the remaining mass after lowering the temperature to 575 ±

25 °C and holding it for 4 hours in an oxygen atmosphere. The ASTM D7582 [32] method was applied to both the feedstock and the produced pellets. A commercial coffee grinder was used to prepare the feedstock samples, while the pellets were analyzed without grinding. The fixed carbon, volatiles, and ash are reported on a dry basis.

A Thermo Flash 2000 elemental analyzer was used to determine carbon and hydrogen content through ASTM E777 [22], nitrogen through ASTM E778 [33] and sulfur through ASTM E775 [34]. The oxygen content was calculated from the difference. An Ankom fiber analyzer was used to determine the composition of the samples through the Van Soest detergent procedure [35]. Neutral detergent fiber (NDF) helped determine the total fiber content. Acid detergent fiber (ADF) provided an estimate of cellulose and lignin, and acid detergent lignin (ADL) was obtained from the treatment of the ADF residue with sulfuric acid. From these results, hemicellulose was obtained as NDF minus ADF, and cellulose was calculated as ADF minus ADL. The high heating value (HHV) of the materials was determined using an IKA C2000 bomb Calorimeter. Considering the heterogeneity of the feedstocks, obtaining representative samples for elemental analysis, the Van Soest detergent procedure, and the bomb calorimeter proved unfeasible. Consequently, these tests were exclusively conducted on the produced pellets. A commercial coffee grinder was used to grind the pellets.

A Kovonovák hammer mill (model SHM-5) with screen sizes of 4, 8, and 12 mm attached to a dust collection system was used to grind the dried materials. A Fluke 3540 FC 3-Phase Power Monitor was used to measure the power consumption during the grinding operation. The three different sizes of ground material are referred to as 4 mm, 8 mm, and 12 mm. The materials were manually fed to the grinder while maintaining a constant load level. The ratio between the material processed and the grinding time is known as the grinding throughput. The fines obtained were

calculated using a mass balance approach, which involved comparing the weights of the ground material and the material fed into the hammer mill. The reported values are the average of three separate measurements. To estimate the bulk density of the ground material, a 5-liter graduated measuring and mixing pitcher was used. The material was poured up to an identifiable volume level, after which the sample was weighed. The reported results represent the average of ten measurements.

ANSI/ASAE S319.3 [36] was followed to evaluate the particle size distribution of the ground samples. Eight mesh sieves of varying aperture sizes were placed in a RO-TAP testing sieve shaker (model B, W.S. Tyler, Ohio, US) for 10 minutes of shaking and taping. The weight of the retained material on each sieve was measured using a weighing scale with a 0.1 g precision. The reported values are the average after three shaking and taping tests for each sample.

2.2.2 Pelletization

The pellets were produced using a flat die pelletizer (model BN4/7/10HP, Kononovák, Citonice, Czech Republic) equipped with a 6 mm type C die and connected to a pellet classifier. A Fluke 3540 FC 3-Phase Power Monitor (Fluke Corporation, Everett, WA, US) was used to measure the power consumption during pelletization. The moisture content of the ground dry material was adjusted by sprinkling water into the mixer compartment of the pelletizer equipped with mixing blades. The blades in the compartment homogenized the mixture for 30 min, and the moisture content of the sample was checked with a moisture tester.

Six combinations of pelletization parameters were tested, including the three particle size types (4, 8, and 12 mm) and two added moisture levels (10 % and 15 %). The pelletizer throughput was regulated by varying the gate valve opening that controls the material flow rate from the mixer to

the pelletizer mill. The fines obtained were determined by the mass balance between the material fed into the mixer, the unprocessed material at the end of the test, and the total weight of the produced pellets. The temperature at the surface of the rollers was measured using an infrared thermometer (Laser grip 800, Etekcity, range: -50 °C to 750 °C) at 1-minute intervals during the pelletization tests.

2.2.3 Pellet quality

The bulk density and durability of the pellets were measured as per ASAE S269.5 [23]. For the bulk density, a 500 mL natural stacking density measurement device was used, and the reported value is the average of three measurements. The durability was measured as the ratio of the weight of the pellets retained on the sieve after the test to the pellet mass before the test. The test consisted of 10 min of tumbling at 50 r/min in a dust-tight enclosure, and the reported durability value is the average of two tests.

The length and diameter of the pellets were measured using a digital Vernier caliper (range: 0-150 mm, accuracy: 0.02 mm), and, to have uniform lengths, the edges of the pellets were smoothed before measurement. The weight of the pellets was measured with a digital balance with an accuracy of 0.01 g. The pellet volume was calculated based on the measured dimensions assuming a cylinder shape. The weight and calculated volume were used to determine the particle density. The reported values are the average of fifteen samples for each pelletization run.

2.3 Results and Discussion

2.3.1 Materials characterization

Table 2 highlights the basic characterization of the materials used in this study. For RDF, the high volatile content is due to the predominant cellulose content of the paper and film plastics. The cellulose content is also higher in RDF than in other feedstocks. For SSO, two batches were analyzed, the first collected during winter and the other during the summer/spring seasons. The proximate, ultimate, and compositional analysis results show a wide variation between the two seasons. The proximate analysis results for the pellets show an increase in the ash content compared to the results for feedstock in both RDF and SSO. The higher ash content in the spring/summer sample is a potential indicator of the presence of soil particles. The seasonal effect can also be noted in the higher amount of lignin for spring/summer that can be associated with the presence of lignocellulosic feed streams in yard waste like twigs and branches from woody resources. The digestate composition shows a high amount of ash and a comparatively low HHV, which in turn could deem digestate a less suitable material for waste-to-energy conversion. The high ash content and low HHV of the digestate contrast with the results reported by Neumann et al. [37] [38] and Kratzeisen et al. [19]; in their work, the digestate was found to have lower ash contents and higher HHVs. However, it is worth mentioning that in those studies the feedstock of the AD process was agricultural residues and animal manure.

Table 2: Thermochemical characterization of materials.

	RDF		SSO Winter		SSO Summer/Spring		Digestate
Moisture as Received (wt %)	4.5 ± 0.5		70.0 ± 1.7		62.9 ± 5.7		62.9 ± 4.9
Proximate analysis							
	Feedstock	**Pellets**	**Feedstock**	**Pellets**	**Feedstock**	**Pellets**	**Feedstock**
Volatiles (wt %)	86.43	80.57	76.86	77.23	60.91	56.02	45.61
Fixed Carbon (wt %)	6.03	9.63	12.03	9.26	10.21	9.25	11.25
Ash (wt %)	7.53	9.80	11.11	13.51	28.88	34.71	43.14
Elemental Analysis							
C (wt %)		45.94		44.64		33.92	29.11
H** (wt %)		6.13		6.46		4.54	3.50
N (wt %)		0.42		2.84		1.98	1.99
S (wt %)		<0.2		<0.2		<0.2	<0.2
O* (wt %)		47.51		46.06		59.56	65.40
Chemical Composition							
Hemicellulose (wt %)		7.90		9.60		9.60	7.70
Cellulose (wt %)		40.40		16.20		12.40	14.50
Lignin (wt %)		34.50		6.60		20.40	31.80
HHV (MJ/kg)		21.5		19.5		13.9	10.1

(*) Calculated by difference.

2.3.2 Grinding energy and particle size

The grinding energy requirement is expressed in terms of specific energy consumption (SEC), which is calculated as the ratio of power consumption to the total mass of processed material during the test. This concept is also used for the pelletization process.

After several grinding and pelletization trials, digestate proved to be not easily pelletizable and no pellets could be produced. Mixing with a binder material could potentially facilitate the pelletization; however, because of the initial results and the marginal energy properties of the digestate, no further tests were conducted with the digestate.
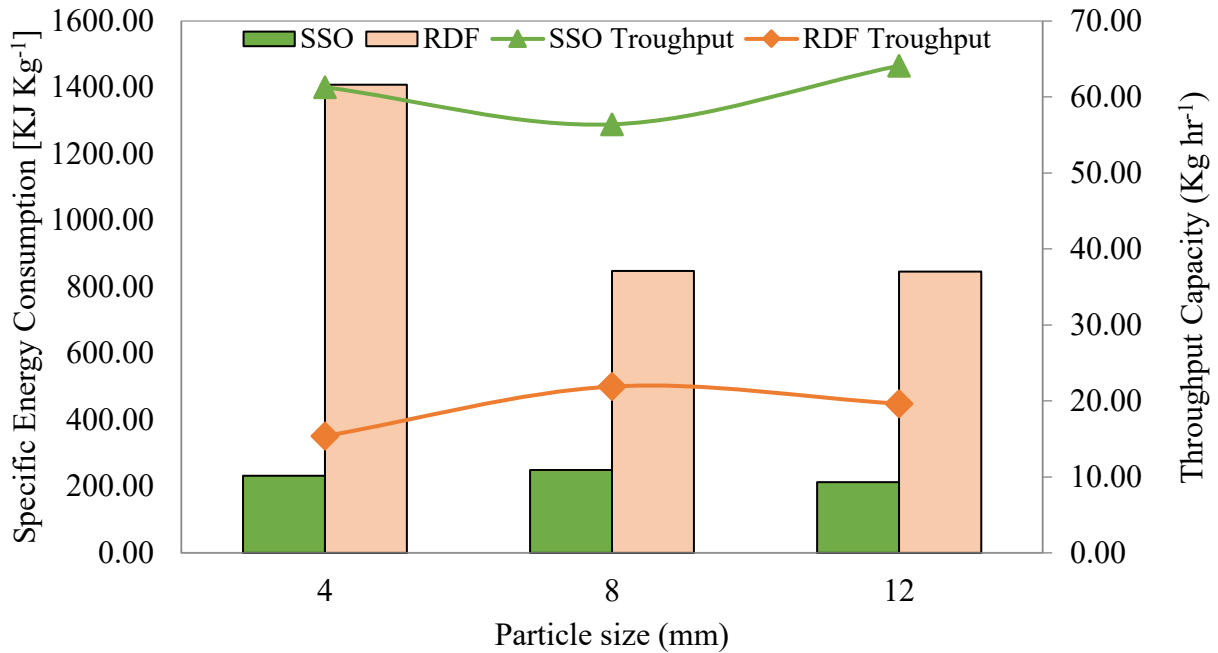
Figure 2: Grinding – Specific energy consumption and throughput

Figure 2 shows the effect of particle size on grinding SEC. The SEC of RDF increases with the use of a 4 mm screen. However, the change is almost negligible between the 8 mm and 12 mm sizes. On the other hand, for SSO, the SEC does not seem to be directly affected by the particle size; the values are comparatively similar among the three sizes. The SEC for grinding is intrinsically related to the material throughput; this relation can be observed when comparing the RDF and SSO since the lower throughput levels achieved for RDF are reflected in higher SEC values. Furthermore, one of the most influential variables in the throughput is the bulk density of the feedstock. The bulk density of ground RDF (29.76 ± 0.80 kg/m^3) is lower than that of ground SSO (342.61 ± 13.4 kg/m^3), indicating the presence of lighter materials in RDF. For RDF at smaller particle sizes, the number of fines suctioned by the dust collection system increases (**Table 3**), while for SSO, there is no apparent effect.

Table 3: Grinding: Fines generation.

Material	Fines generation (wt %)		
	4 mm	8 mm	12 mm
RDF	22.4	15.0	9.3
SSO	2.1	7.4	3.4

The particle size results are presented following ISO 9276-1 [39]. For instance, the P_{50} value represents the particle size diameter at 50 % in the cumulative undersize particle distribution. **Figure 3** shows the particle size distribution of RDF and SSO. Because of differences in material, the P_{50} sizes for RDF completely depend on the grinding screen; the 4, 8, and 12 mm show sizes of 1.49, 4.18, and 5.86 mm, respectively. On the other hand, the brittle nature of SSO reduces the effect of the grinding screen on the P_{50} value. Nonetheless, the size distribution range is wider for the 12 mm size. Overall, there is a broader size range for RDF than for SSO. The biggest particles observed in SSO are in the 3.5 mm range, and in RDF in the 12 mm range.
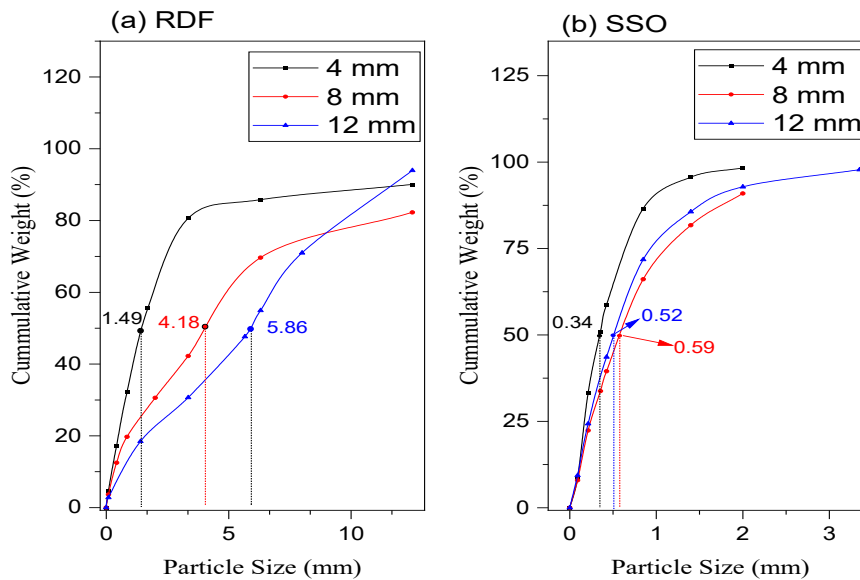
Figure 3: Particle size distribution. a: Ground RDF; b: Ground SSO

2.3.3 Pelletization

Figure 4 shows the specific energy consumption (SEC) and throughput results of the pelletization process for RDF and SSO under the six combinations of particle sizes and moisture contents. For both materials, the particle size has a direct effect on the SEC and an inverse relation with the throughput. The RDF 8 mm 15 % is the only outlier for this trend. The moisture content has a direct relation with the SEC for SSO, while for RDF there is an inverse relation.
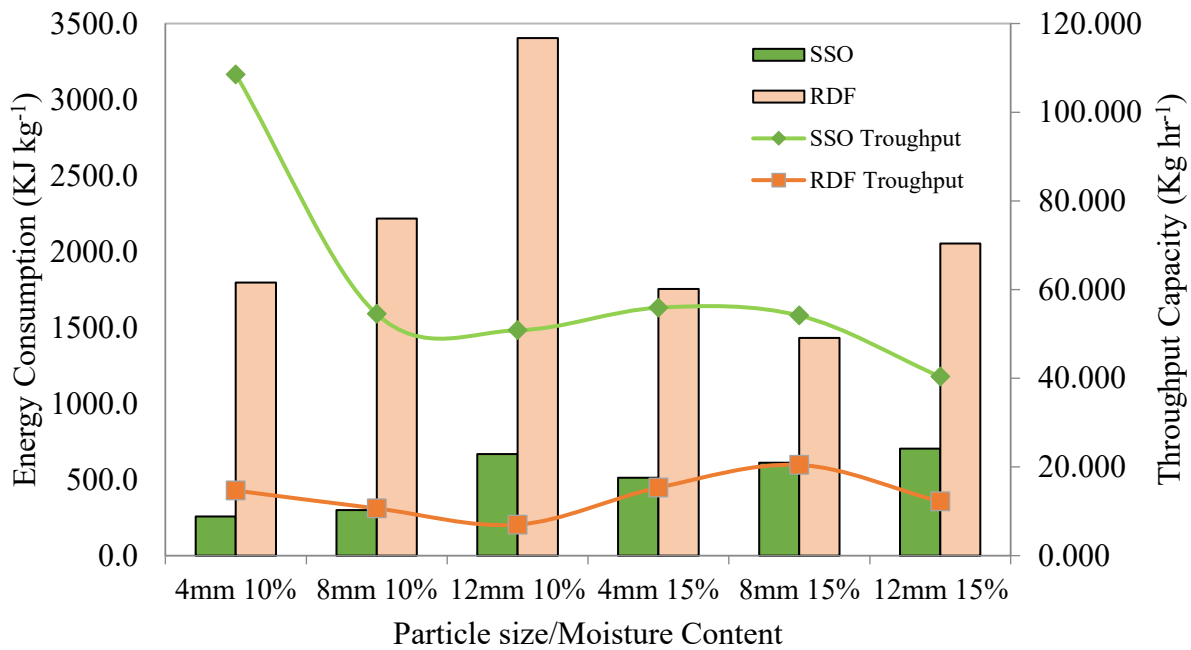
Figure 4: Pelletization – Specific energy consumption and throughput

Table 4 shows the fines generated during pelletization. For RDF, both particle size and moisture content have a direct effect on fines generation. For SSO, there is no evident effect of particle size in fines generation; however, the fines are lower at higher moisture contents. These results contrast with the findings of Pradhan et al [40] in their work with garden waste; these authors found that fines generation increased with milling size but showed no clear relationship with moisture

content. The fines generation from RDF was higher than from SSO for every particle size and moisture content combination.

Table 4: Pelletization: Fines generation.

Material	Fines generation (wt %)					
	4 mm 10 %	8 mm 10 %	12 mm 10 %	4 mm 15 %	8 mm 15 %	12 mm 15 %
RDF	21.1	23.4	33.1	23.7	38.5	39.7
SSO	12.8	6.1	11.0	6.2	6.4	6.9

Figure 5 shows the temperature profile of the pelletizer mill. It was observed that the temperature of the pelletizer mill stabilized after a few minutes. Hence, the reported value is the average of the measurements taken during the second half of each experiment. This step can be assumed to be a steady-state pelletization interval. The maximum standard error in the temperature measurements was 4.6 %. There is a direct relationship between particle size and temperature, one that is more noticeable for SSO. For RDF, the temperatures achieved during the process are lower than those reported in the literature (80 °C to 120 °C) [18, 23, 25]. The results obtained differ from the finding of Jewiars et al. [25], for instance, in that it was found that RDF pellets of acceptable quality could be produced at temperatures below 80 °C. However, Jewiars et al. worked with pellet diameters in the range of 12 mm to 20 mm, while our pellets have a diameter of 6 mm. The difference in the process temperature requirements could be associated with the effect of the die diameter.
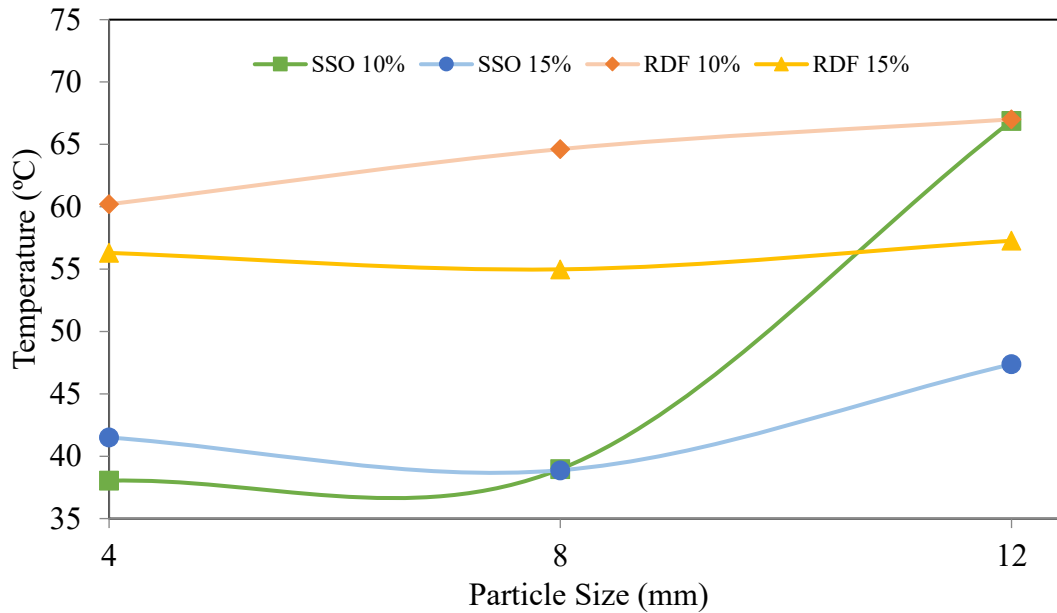
Figure 5: Pelletization temperature

2.3.4   Pellet quality

Figure 6 shows images of the produced pellets. **Figure 7** show particle density, bulk density, and moisture content of the conditioned material. It was observed that moisture content and particle size do not have any effect on the bulk and particle densities of RDF. A maximum bulk density of 594 kg/m^3 was achieved in RDF at a screen size of 8 mm with 10 % moisture. A maximum particle density of 1002.8 kg/m^3 was achieved at a screen size of 12 mm with 10 % moisture. The variation in the bulk and particle densities for the six different pelletization combinations was limited to 5.5 % and 6.3 %, respectively. The particle and bulk densities of SSO with 10 % moisture content increase with particle size. This trend was not observed in the 15 % moisture content combination. SSO at a screen size of 12 mm with 10 % moisture produced pellets with the highest bulk and particle densities of 730.7 kg/m^3 and 1285 kg/m^3, respectively. The range in bulk and particle densities for the different combinations was limited to 9.95 % and 11.98 %, respectively.

Figure 6: Produced pellets. Left: SSO pellets; Right: RDF pellets. Both at 4 mm and 10 %.

For RDF pellets, a drop in the moisture content was observed between the conditioned (added moisture) feedstock and the pellets. The moisture reduction average for the six combinations was 7.63±0.66 %. In contrast, the measured moisture of the conditioned SSO varied among the expected values. This shows a higher complexity in the conditioning of the SSO, although an average moisture reduction of 4.33±1.78 % was observed in the SSO pellets. The difference in moisture loss during pelletization can be associated with the process temperatures described previously. The highest moisture loss levels of 7.71 % for SSO and 7.89 % for RDF occurred at the combinations with the highest process temperatures at a screen size of 12 mm and 10 % moisture for both SSO and RDF.
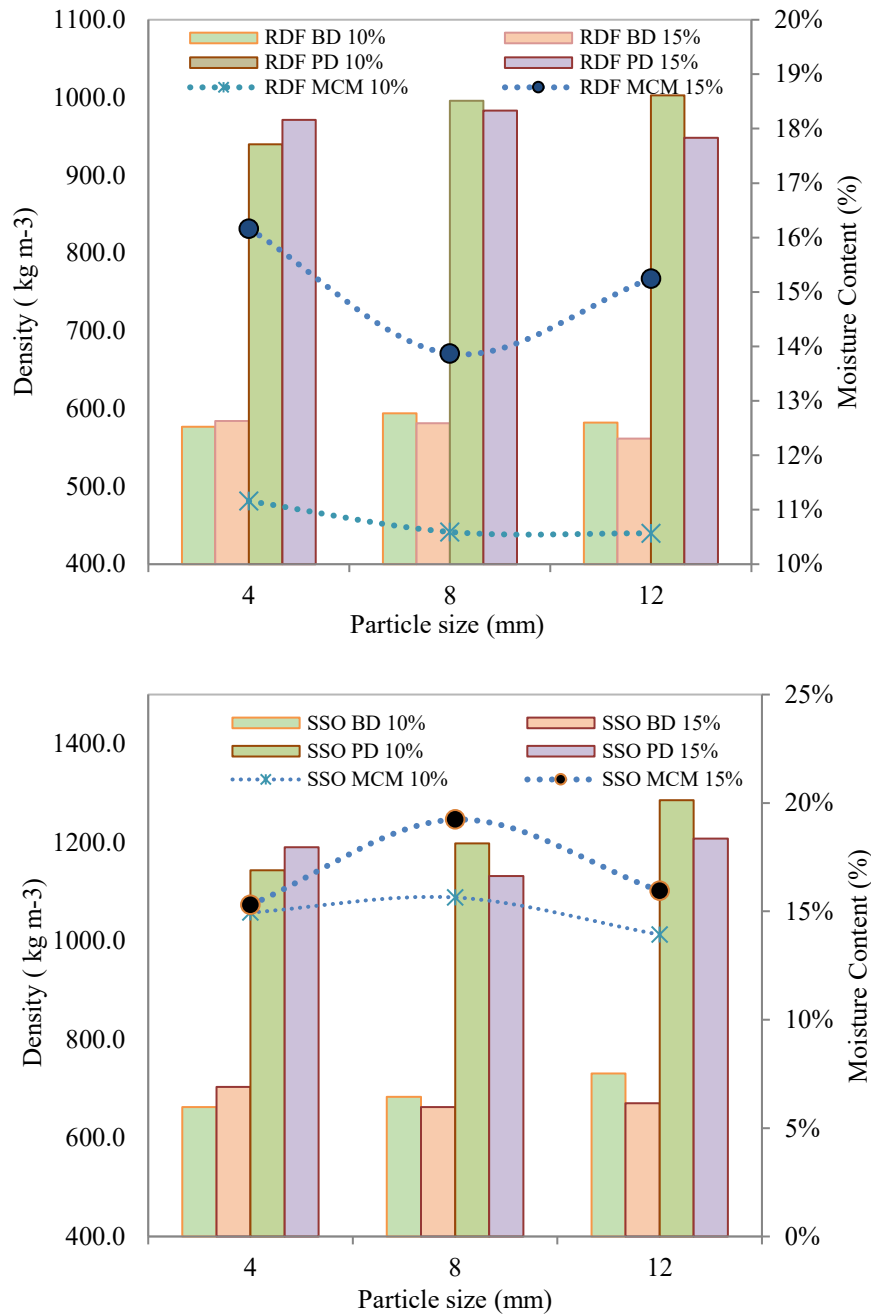
Figure 7: RDF and SSO pellets bulk density (BD), particle density (PD) and moisture of conditioned material (MCM)

Figure 8 shows the durability of the pellets. For RDF, feedstock with 10 % MC produced better durability pellets than the feedstock with 15 % MC; however, no relationship was observed with particle size. A trend was observed in which the RDF pellets with lower moisture content had higher durabilities. For SSO, no relationship can be directly observed between pellet durability

and the moisture content of the feedstock. Nonetheless, there is an evident direct relationship with the moisture content of the produced pellets. The highest durability of 97.4 % was achieved for the 8 mm 15 % MC combination, which also produced the pellets with the highest moisture content of 14.48 %. Agar et al. [18] reported a similar relationship in their work with woody residues. This phenomenon occurs as a result of the hydrogen bonding between biomass particles due to the enhancing effect of water [41] .
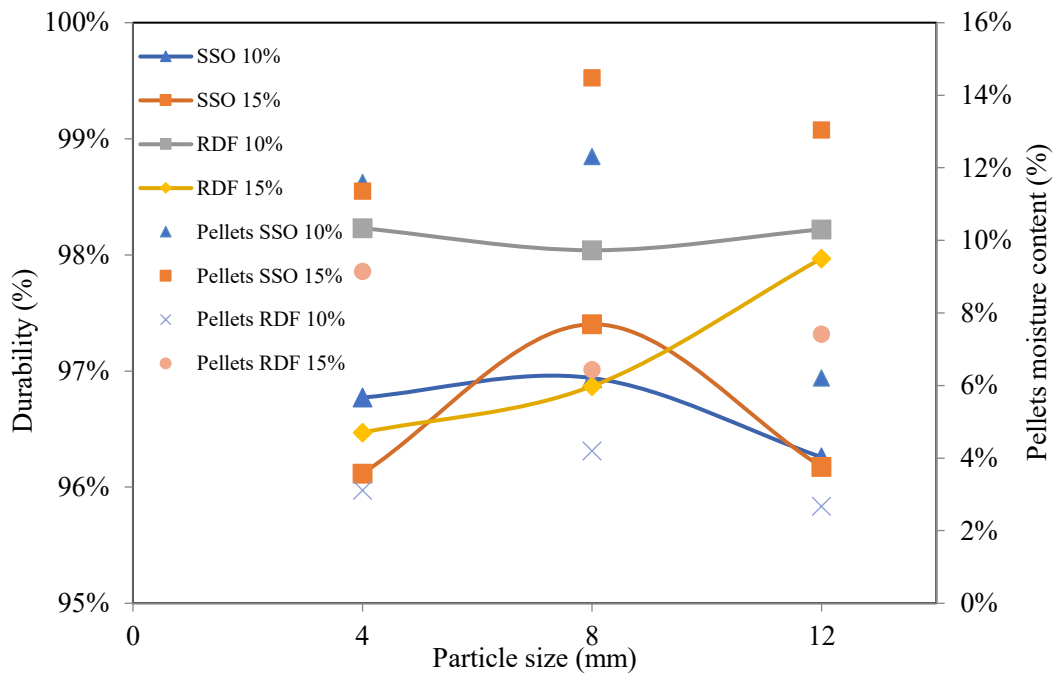
Figure 8:Pellet durability and moisture

Table 5 shows the length and diameter of the produced pellets. The maximum standard error in the length measurements was 0.96 mm, and 0.04 mm for the diameter. Both materials had clear relationships between particle size and pellet length, but no relationship was observed with moisture content. However, there was a clear relationship between the RDF pellet's diameter and moisture content. Pradhan et al. [40] reported a similar observation in the pellets produced from garden waste. This phenomenon was seen in high MC materials where the swelling was due to the release of water vapours present in the warm pellets. In general, SSO pellets presented lower

dimensional variability. The average standard deviation for SSO and RDF pellets' length was limited to 2.39 and 3.21 mm, respectively. In terms of the diameter, the average standard deviation of SSO pellets was 0.11 mm, compared to 0.44 mm for the RDF pellets.

Table 5: RDF and SSO pellet length and diameter.

Material	Dimension	4 mm 10%	8 mm 10%	12 mm 10%	4 mm 15%	8 mm 15%	12 mm 15%
RDF	Length (mm)	15.52	15.77	19.54	16.43	16.57	16.93
	Diameter (mm)	6.06	6.05	6.05	6.09	6.13	6.13
SSO	Length (mm)	19.16	19.77	20.04	17.95	19.05	20.83
	Diameter (mm)	6.37	6.27	6.02	6.29	6.21	6.05

2.3.5 Overall quality assessment

To perform an overall quality assessment of the pellets, a comparison matrix was developed following the quality specifications defined by ISO 17225-6 [42]. Bulk density, moisture, and durability were considered in the comparison; length and diameter were not included because all the pellets met these requirements. Ash content was also excluded, as the proximate analysis results showed minimal variation between the different combinations of the same material. ISO 17225-6 defines 10 % mass dry as the maximum acceptable ash content. RDF pellets are just within the limit with an average of 9.8 %, while SSO pellets, with an average of 34.71 %, are far above the established limit. The total specific energy consumption, defined as the sum of the grinding and pelletization energies, is also considered in the comparison matrix. The throughput capacities are not considered, as the SEC values consider their effect. **Table 6** shows the pellet quality comparison matrix. For each variable, a score of 6 was assigned to the combination with the best value and 0 for the one with the worst. A "Total Score" was calculated as the sum of all the scores in the different comparison variables. For RDF, the best combination is the 8 mm screen

size with 10 % MC. For SSO, two combinations share the highest score, the 8 mm screen size with 10 % MC and the 12 mm screen size with 10 % MC. The 12 mm screen size with 10 % MC combination has the highest bulk density and lowest moisture, while the 8 mm screen size with 10% MC has better durability and lower specific energy consumption. These results can be used as initial guidelines for further research on the scale-up of the pelletization process.

Table 6: Pellet quality comparison matrix.

	Bulk Density	Moisture	Durability	SEC	Total
ISO 17225-6	≥ 550 kg/m³	≤ 15 %	≥ 96 %	NA	
RDF 4 mm 10 %	2	5	6	2	15
RDF 8 mm 10 %	6	4	4	4	18
RDF 12 mm 10 %	4	6	5	1	16
RDF 4 mm 15 %	5	1	1	3	10
RDF 8 mm 15 %	3	3	2	6	14
RDF 12 mm 15 %	1	2	3	5	11
SSO 4 mm 10 %	2	4	4	6	16
SSO 8 mm 10 %	4	3	5	5	17
SSO 12 mm 10 %	6	6	3	2	17
SSO 4 mm 15 %	5	5	1	4	15
SSO 8 mm 15 %	2	1	6	3	12
SSO 12 mm 15 %	3	2	2	1	8

2.4 Conclusions

The results of this pelletization study showed that grinding was effective for controlling the particle size distribution of RDF, while its effect on SSO is low. The pelletization of RDF and SSO is feasible; however, the digestate generated at the EWMC could not be pelletized. The alternative of mixing it with a binder could be explored in future research. With 62.98 % moisture, an ash content of 43.1 %, and a calorific value of 10.1 MJ/kg, the digestate generated in the City of Edmonton might not be suitable for densification.

The produced RDF pellets with an HHV of 21.5 MJ/kg have good potential for waste-to-energy conversion given their low ash and high volatiles content. The ash content in SSO (13.51 % in winter, 34.71 % in summer/spring) is higher than what is considered acceptable for solid biofuels; also, there is a seasonal variation in the composition of SSO. Further research is therefore required to identify the seasonal variation pattern of the different waste streams.

For both SSO and RDF, the particle size has a direct influence on the specific energy consumption and the pelletization temperature, while it has an inverse relation with the process throughput. The moisture content showed a direct relation with the pelletization energy requirement for SSO, but the relation is inverse for RDF. The findings of this study will serve as a benchmark for future researchers working on the pelletization of SSO and RDF at a pilot scale.

All the particle size and moisture content combinations delivered pellets with acceptable properties for both materials. The lower moisture combinations produced higher durability RDF pellets. The final moisture content of SSO pellets has a direct relationship with their durability. However, neither particle size nor moisture content showed an identifiable effect on the bulk or particle density of RDF pellets. However, particle size directly affects the bulk and particle density of SSO pellets.

Based on a quality assessment matrix, for SSO, the 12 mm screen size with 10 % MC combination produced the best quality pellets, while for RDF, two combinations, the 8 mm and 12 mm screen sizes, both with 10 % MC, produced the highest quality pellets. The information developed can help in pelletization of MSW and its scale up for production of energy.

Chapter 3: The thermo-catalytic reforming of the source-separated organics generated in an urban municipality located in a colder region

3.1 Introduction

The production and use of clean fuels are key components of the transition to a low carbon emission future. Clean fuels include advanced biofuels, renewable natural gas, hydrogen, sustainable aviation fuel, and synthetic fuels. The International Energy Agency (IEA) projected that by 2050, up to 51 % of Canada's energy demand will be met by clean fuels. This presents a significant growth opportunity, as currently clean fuels account for only 6 % of energy demand [43]. Among the alternatives available, biomass conversion using pyrolysis is a promising method to produce clean fuels.

Pyrolysis is a thermochemical conversion method that transforms biomass feedstock into value-added products. The process requires heating the biomass in an oxygen-free atmosphere, thereby decomposing the organic matter and converting it into bio-oil, an aqueous phase, syngas, and biochar [44, 45]. Pyrolysis can be classified as slow, intermediate, and fast, depending on factors such as process temperature, heating rates, and residence time. Intermediate pyrolysis takes place at temperatures of 400-550 °C with moderate heating rates of 200-300°C/min and vapour residence times of 2-4 seconds [9]. The thermo-catalytic reforming (TCR) technology developed by Fraunhofer UMSICHT [10] uses an intermediate pyrolysis auger reactor followed by a catalytic reforming process that improves the quality of the pyrolysis products [11]. The main variables to be controlled in the TCR process are the pyrolysis reactor and reformer temperatures. The

operating temperature range of the pyrolysis reactor is 400°C to 600°C, while the reformer temperatures can range from 400°C to 750°C [46].

Research using TCR has been done with various biomass feedstocks including forest [47] and agricultural residues [48], digestate [37][38], sewage sludge [49], and municipal solid waste (MSW) [12,13], among others. Hornung et al. [50] demonstrated the primary benefits of TCR technology and how it can be combined with others to create marketable products while reducing its substantial waste streams.

Kurian et al. [46] showed how feedstock composition influences product yield. Bio-oil production is mainly affected by the presence of hemicellulose and cellulose, while lignin content is linked to the production of biochar. Gill et al. [47] reported a maximum bio-oil yield for woody biomass at a combination of 500 °C pyrolysis and 600 °C reforming temperatures. Kurian et al. also found that increasing the reformer temperature reduces the yields of biochar and bio-oil while increasing the production of syngas [46].

Municipal solid waste (MSW) refers to the waste generated by households, commercial establishments, and institutions within a municipality or urban area. This includes items like household garbage, packaging materials, food waste, and more. In Edmonton, Alberta, waste collection is organized into three streams based on the type of residue: organics and garden waste, ordinary residues, and recyclables. The Edmonton Waste Management Centre (EWMC located at 53°35'02.0"N 113°36'49.7"W) handles each stream separately. The organics and garden waste, referred to as source-separated organics (SSO), are shredded and then used as feedstock in the anaerobic digestion (AD) process.

Ouadi et al.[12] studied the use of TCR to convert MSW. The light fraction of the MSW (mainly plastic and paper) was obtained from a solid recovered fuels plant to be pelletized and processed in the TCR. With a pyrolysis temperature of 450 °C and reformer temperature of 700 °C, the bio-oil yield was 6 % with a high heating value (HHV) of 38 MJ/kg. The syngas and biochar yields were 44 % and 31 %, respectively. The syngas had a H_2 concentration of 36 vol% and an HHV of 17.23 MJ/Nm^3.

Kirby et al. [13] used the organic fraction of municipal solid waste as feedstock for TCR. At a fixed pyrolysis temperature of 450 °C and reforming temperatures of 450 °C, 600 °C, and 700 °C, product yields ranged from 2.7 % to 5.9 % for bio-oil, 13.6 % to 36.2 % for syngas, and 39.6 % to 45.9 % for biochar. The highest calorific values for bio-oil, syngas, and biochar were 39.0 MJ/kg, 16.9 MJ/kg, and 6.8 MJ/kg, respectively.

To the extent of our knowledge, there are no other characterizations of TCR products using the organic fraction of the MSW; moreover, the aforementioned studies were conducted using MSW generated in Europe. Furthermore, since the composition and characteristics of MSW streams vary depending on location, waste management policies, source separation practices, and municipal treatment facilities [22] [51], assessing the suitability of the SSO waste stream for thermochemical conversion requires a localized approach.

This study aimed to investigate the use of pelletized source-separated organics (SSO) for thermochemical conversion through the TCR process. The feedstock used in this study was sourced from Edmonton, Alberta, in Canada. The effect of the pyrolysis and reformer temperatures on the yield of bio-oil, biochar, and syngas was explored. Also, the influence of process temperatures on the characteristics of the products was investigated. The overarching goals were

to generate valuable information that can be used to assess the feasibility of scaling up the technology and determine upgrading requirements for product commercialization.

3.2 Materials and Methods

3.2.1 Materials

The SSO feedstock collected during the spring/summer seasons from the Edmonton Waste Management Centre (EWMC) was dried and pelletized. The resulting pellets, with a diameter of 6 mm, had a bulk density of 662 to 730 kg/m^3, an average moisture content of 10 %, and a durability above 98 %. Additional physical and chemical details of the feedstock and resulting pellets are given later in the document.

3.2.2 Experimental setup

A thermo-catalytic reforming device with a feed rate of 2 kg per hour (known as a TCR-2) was used to process the SSO pellets. **Figure *9*** shows the main components of the system. The entire system operates under an inert N$_2$ atmosphere. The feedstock is initially loaded into a hopper mounted on top of the system. At the bottom of it, there is a feeding screw driven by an electric motor to supply the feedstock at a controlled rate. The feedstock falls into the intermediate pyrolysis reactor equipped with 3 electric heaters located along the reactor length. The first heater is maintained at 350°C and the other two can be set at temperatures of 400-500 °C. Two internal augers move the feed along the reactor while mixing fractions of the char and the incoming feed. Once inside the reactor, pyrolysis occurs at a heating rate of 1 °C/s and an average residence time of 12 min. The next stage in the process takes place in the post-reformer, which is heated to a temperature of 500°C to 700 °C. The vapours released during the reaction flow through the internal pipes of the reformer and the char accumulates at the bottom. The char acts as a catalyst to generate the post-reforming effect on the vapours [12,52]. The upgraded vapours are then condensed in two

consecutive shell-and-tube heat exchangers cooled by chilled water. The mix of condensed bio-oil and the aqueous phase is collected in a glass bottle located at the bottom of the condensers. The syngas flows through a scrubber and then is filtered to remove traces of liquid. Part of the syngas is diverted to a portable gas analyzer at the outlet. The entire system is operated and monitored through an electronic interface, which is equipped with temperature and pressure sensors, as well as flow meters. The operating temperatures of the system are controlled with eight electric heaters. The feedstock supply starts once the desired temperatures have stabilized.
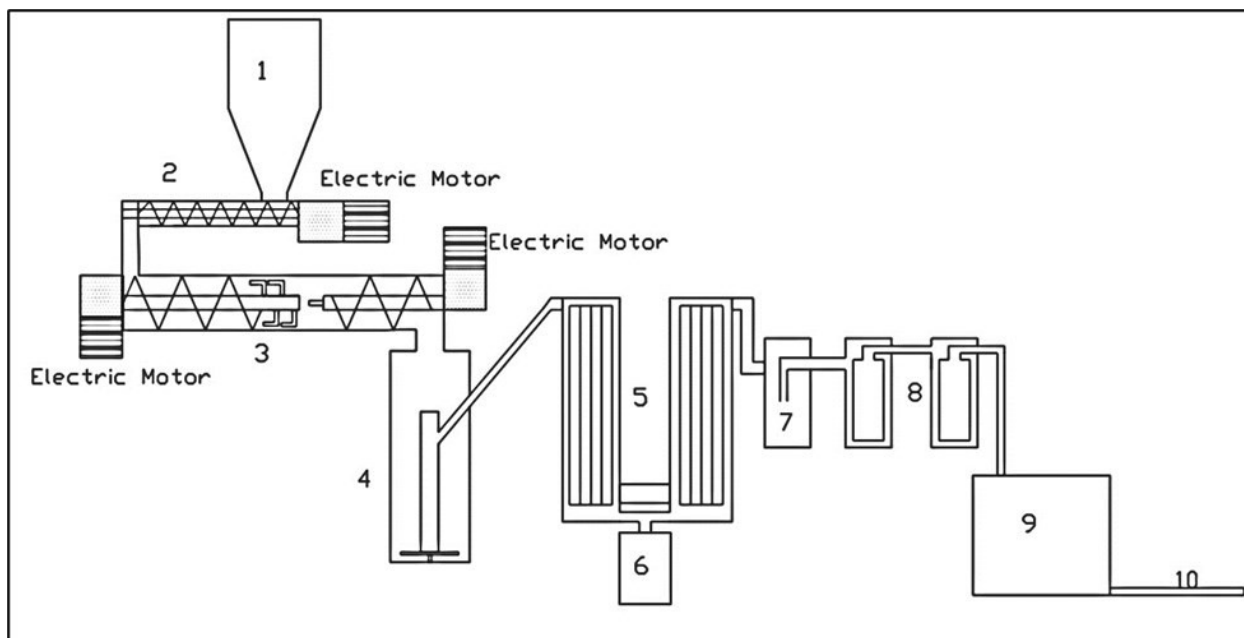
Figure 9: TCR-2 process schematic. 1. Feed hopper, 2. Feeder screw, 3. Pyrolysis reactor, 4. Post-reformer, 5. Gas condensers, 6. Aqueous phase container, 7. Gas scrubber, 8. Gas filters, 9. Gas analyzer. Taken from my research colleague B. Dhakal's thesis [48]

3.2.3 Operating parameters

To understand the effects of process temperatures on the yield and characteristics of the products, six experiments were conducted at pyrolysis reactor temperatures of 400 °C and 500 °C and post-reformer temperatures of 500 °C, 600 °C, and 650 °C.

All six experiments had consistent feeding rates and reactor screw speeds. The feeder motor operated in 2 seconds on / 13 seconds off intervals to ensure a feedstock flow rate of approximately 2 kg/hr. The reactor screw motors were adjusted to achieve a residence time of approximately 12 min.

3.2.4 Analytical methods and measurements

The condensed bio-oil and the aqueous phase fraction was transferred to a separating funnel and held for 24 hours to facilitate the decantation process. After the equipment had cooled down, the biochar was removed from the bottom of the reformer.

3.2.4.1 Biochar analysis

The proximate analysis of biochar was performed according to ASTM D7582 [32] using a LECO TGA701 thermogravimetric analyzer to determine the moisture, fixed carbon, volatiles, and ash content. Initially, the moisture content was calculated by keeping the sample at 106 °C until constant readings were obtained. The volatiles and fixed carbon content were calculated by heating the samples to 900 °C at a holding time of 15 minutes and a heating rate of 40°C/min in an inert atmosphere. The ash content was determined from the remaining mass after lowering the temperature to 575 ± 25 °C and holding it for 4 hours in an oxygen atmosphere. The fixed carbon, volatiles, and ash are reported on a dry basis.

Ultimate analysis was done using a Thermo Flash 2000 elemental analyzer. ASTM E777 [53] was followed for Carbon (C) and hydrogen (H) [22], ASTM E778 [33] for Nitrogen (N) [20], and ASTM E775 [34] for Sulfur (S). The oxygen (O) content was calculated from the difference. The analysis was performed by subjecting the sample to dynamic flash combustion at high temperature in a controlled oxygen environment. The resulting gases were analyzed using the gas

chromatographic separation method [54]. An IKA C2000 Bomb calorimeter was used to determine the high heating value (HHV). The sample was burned in a high-pressure oxygen atmosphere under adiabatic conditions. The heat generated by the combustion was transferred to the calorimeter's water jacket. The temperature rise of the water was measured and used to calculate the calorific value of the sample [55].

3.2.4.2 Condensate analysis

The elemental composition and calorific value (HHV) of the bio-oil were determined following the procedures detailed in the previous section. The water content of bio-oil was analyzed using a Mettler Toledo™ V20S Volumetric KF Titrator by following ASTM D4377 [56] and using tetrahydrofuran (THF) as solvent [57]. The sample was dissolved in THF and added to the Karl Fischer reagent. The electrical current produced by the reaction was measured with the electrode. The amount of charge required to reach the titration endpoint is proportional to the water content in the sample. The total acid number (TAN) was determined with a Mettler Toledo T50 Titrator as per ASTM D664 [58]. The sample was dissolved in a titration solvent and titrated with alcoholic potassium hydroxide using a combination electrode. Endpoints were determined based on well-defined inflections in the resulting curve. The viscosity of the bio-oil was measured using an Anton Paar rotational rheometer – RheolabQC – following DIN 53019-1 [59]. Viscosity measurements were conducted at 20 °C and 40 °C.

The density of the bio-oil was determined using an Anton Paar DMA 4500M benchtop density meter that operates following ASTM D4052 [60]; the density was measured at 20 °C. The reported density is the average of 3 readings.

An Agilent GCD 1800A (Column = Rtx-5MS 30 m x 0.25 mm, df = 0.25 microns), a gas chromatograph (GC) attached to a mass spectrometer (MS), was used to analyze the bio-oil composition. The heating profile of the GC column starts at 40 °C with a hold time of 2 min followed by heating at a rate of 10 °C/min to reach 280 °C at a hold time of 10 min. An aliquot of the sample was analyzed using ChemStation software, and the compounds were identified using the NIST Mass Spectral Library. The compounds' quantities are expressed in terms of the relative abundance of the peak area.

The density of the aqueous phase was measured following the method detailed above. The pH was determined using an OAKTON Instruments Portable pH 6+ Meter kit. The reported values are the average after 3 measurements.

3.2.4.3 Syngas analysis

A Wuhan Tianyu Intelligent Control Technology Co. portable syngas analyzer (model TY6330P) was used to determine the syngas composition. The measurement accuracy of the analyzer is presented in **Table 7**. The reported gas compositions are the normalized values after deducting the nitrogen (N_2) readings. The calorific value (HHV) of the syngas was estimated as per **Equation 1**. The individual heating values were obtained from Waldheim and Nilsson [61]; densities at atmospheric pressure and concentration % of the gases were considered for the calculation by following the method proposed by Sheng et al. [62]. The properties of propane (C_3H_8) were assumed to estimate the values related to the C_nH_m fractions. The reported results correspond to the average gas composition during the last 2 hours of each experiment, with data collection every 15 min.

Table 7: Portable gas analyzer specification

Component	Method	Range (%)	Resolution (%)	Precision (%)
CO_2	NDIR	0 - 5 to 100	0.01	≤ 2
CO	NDIR	1 - 5 to 100	0.01	≤ 2
H_2	TCD	2 - 5 to 100	0.01	≤ 3
O_2	ECD	3 - 5 to 25	0.01	≤ 3
CH_4	NDIR	4 - 5 to 100	0.01	≤ 2
C_nH_m	NDIR	5 - 5 to 10	0.01	≤ 2

$$HHV \ of \ Syngas \ (MJ/kg) = HHV of \ H_2 \ + \ HHV of \ CH_4 \ + \ HHV of \ CO + HHV of \ C_3H_8 \qquad (1)$$

where,

$$HHV of \ H_2 \ = 12.76 \ x \ Vsyngas \ x \ \% \ of \ H_2 \ (MJ/kg) \qquad (1a)$$

$$HHV of \ CH_4 \ = 39.82 \ x \ Vsyngas \ x \ \% \ of \ CH_4 \ (MJ/kg) \qquad (1b)$$

$$HHV \ of \ CO = 12.63 \ x \ Vsyngas \ x \ \% \ of \ CO \ (MJ/kg) \qquad (1c)$$

$$HHV of \ C_3H_8 \ = 88.44 \ x \ Vsyngas \ x \ \% of \ C_3H_8 \ (MJ/kg) \qquad (1d)$$

3.3 Results and Discussion

3.3.1 Product distribution

The product yields reported on a mass percentage basis are shown in **Figure 10Figure 10**. The yields of bio-oil, biochar, and the aqueous phase decrease as the reformer temperature increases. In contrast, the syngas yield, calculated by the difference, increases as the reforming temperature increases. The reduced bio-oil yield is related to the enhanced cracking of the organic vapours promoted by higher reforming temperatures. This is also reflected in a higher yield of permanent gases [63]. In parallel, the reduced aqueous phase yield can be associated with the water-gas shift reaction that favors the production of carbon dioxide and hydrogen as the result of the reaction between water and carbon monoxide at higher temperatures [63]. This behaviour is consistent with the findings of Gill et al. [47] in the TCR conversion of woody feedstocks as well as those of Neuman et al. [63] with digestate. The bio-oil yield varied from 2.11 % to 6.2 %, with the highest yield achieved at temperatures of 500 °C in the reactor and 500 °C in the reformer. The lowest aqueous phase yield of 13.24 % was obtained at 500 °C in the reactor and 650 °C in the reformer; accordingly, for these temperatures, a maximum yield of 42.79 % was achieved for syngas. The biochar yield fluctuated between 46.25 % and 41.17% for the different temperature combinations. A slight increase in syngas yield was observed with the increase in the reactor temperature, suggesting a greater amount of cracking occurring during pyrolysis [48]. However, the effect of reactor temperature on the yields of bio-oil, biochar, and the aqueous phase does not show a clear trend.
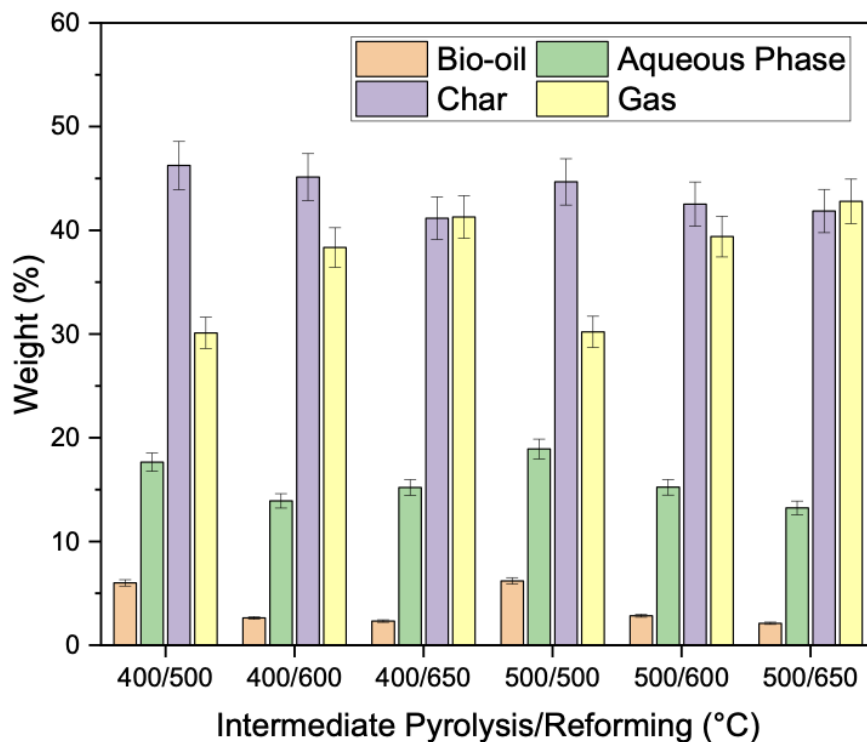
Figure 10: Product yield distribution.

3.3.2 Biochar characterization

Table 8 shows the ultimate and proximate analysis results of the generated biochar at the different process temperatures. The volatiles, nitrogen content, and HHV show a clear decreasing trend with increasing reforming temperatures. The HHV of the char is lower than the values reported by Ouadi et al. [12] for MSW (17.0MJ/kg) but higher than those reported by Kirby et al. [13] for char produced from the organic fraction of MSW (7.5 MJ/kg). No clear relationship can be observed between the process temperatures and the carbon (C) content. This differs from the findings of Neumann et al. [63] who observed an increase in the carbon content with increased reforming temperatures. Ash content ranges from 64.9 % to 70.9%, which is higher than the 44.9 % reported

by Ouadi et al. [12] for MSW. This can be explained by the higher ash content present in the feedstock used in this study.

Table 8: Biochar characterization

T Reactor / T Reformer (°C)	400/500	400/600	400/650	500/500	500/600	500/650	SSO Pellets
Proximate Analysis (Volatiles, Fixed carbon, Ash)							
Volatiles (wt %)	10.69	9.42	8.23	9.88	7.16	6.67	56.00
Fixed carbon (wt %)	24.39	23.71	25.56	23.61	23.56	22.42	9.20
Ash (wt %)	64.93	66.88	66.21	66.51	69.30	70.91	34.70
Elemental Analysis (CHNSO)							
C (wt %)	29.50	29.77	29.04	29.83	26.12	27.31	33.92
H** (wt %)	1.5	1.5	1.5	1.5	1.5	1.5	4.54
N (wt %)	1.26	1.07	0.97	1.21	0.85	0.77	1.98
S (wt %)	<0.2	0.20	0.23	<0.2	<0.2	0.21	<0.2
O* (wt %)	67.54	67.46	68.26	67.26	71.32	70.21	62.40
HHV (MJ/kg)	10.24	9.96	9.67	10.53	9.50	9.25	13.90

* Calculated by the difference.
** Minimum readable value by the equipment.

3.3.3 Syngas composition

Figure 11Figure 11 shows the range in syngas composition at different process temperatures as well as the estimated HHV of the syngas. Increasing the reforming temperature directly affects the percentage of methane, carbon monoxide and hydrogen, whereas the concentration of carbon dioxide and heavier hydrocarbons shows an inverse effect. The increase in gas yield at higher reforming temperatures, along with the rise in the concentration of energy-containing gases, improves the HHV. This behaviour can be explained by Equation 1(a) to (d). It is worth mentioning that the effect of the increased concentration of hydrogen, methane, and carbon monoxide outweighs the reduced concentration of higher hydrocarbons. The highest syngas HHV (19.13 MJ/kg), along with the highest concentrations of hydrogen (36.36%), methane (11.05%), and

carbon monoxide (15.63%), were obtained at a reactor temperature of 500 °C and a reformer temperature of 650 °C. The reported maximum HHV is higher than the 17.0 MJ/kg reported by Kirby et al. [13] in their work on the organic fraction of MSW and higher than the 17.23 MJ/Nm^3 reported for Syngas produced from MSW by Ouadi et al. [12]. The hydrogen concentration change can be caused by the water-gas shift reaction between water and carbon monoxide to produce hydrogen [63]. Carbon dioxide is reduced by the Boudouard reaction in which CO_2 and carbon are converted to carbon monoxide [38]. The increase in the concentrations of methane and carbon monoxide at higher reforming temperatures differs from the findings reported by Dhakal [48] and Neumann et al. [38]\, who found that methane and carbon monoxide steadily decrease at higher reforming temperatures.
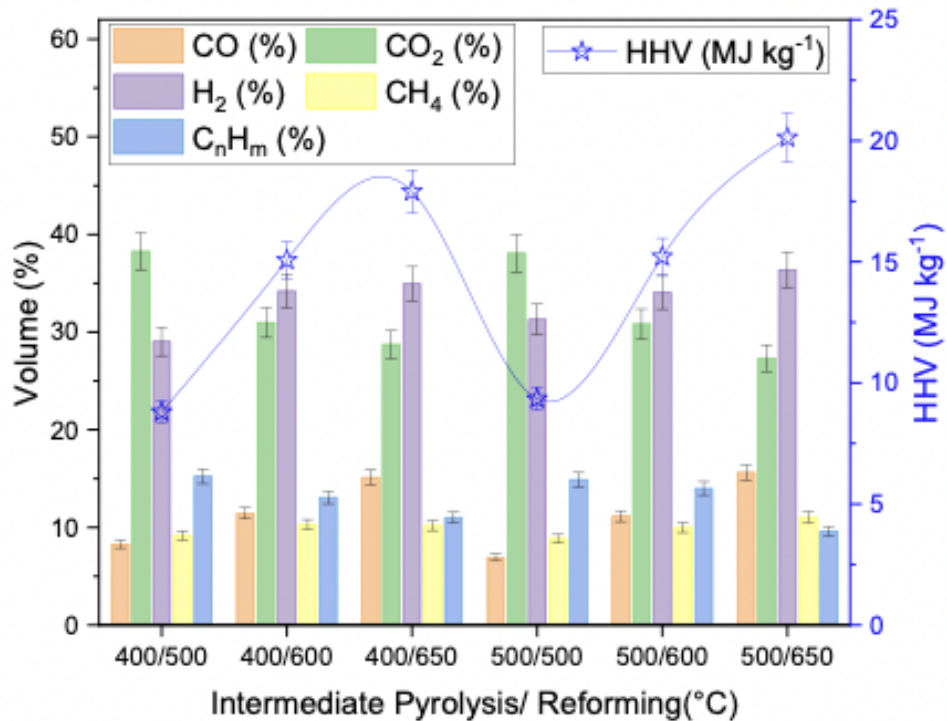

Figure 11: Gas composition and HHV variation.

3.3.4 Condensate characterization

The thermochemical characterization of the produced Bio-oil is presented in **Table 9.** The biodiesel characterization, from Hossain et al. [64] is included as a reference. Both hydrogen and sulfur content show a decreasing trend at higher reforming temperatures, whereas nitrogen shows an increasing trend.

Table 9: Bio-oil characterization

T Reactor/T Reformer (°C)	400/500	400/600	400/650	500/500	500/600	500/650	Biodiesel[**]
C (wt %)	77.06	78.05	79.00	78.65	76.55	80.19	77.2
H (wt %)	8.58	7.02	6.59	8.56	6.72	6.21	13.2
N (wt %)	5.01	6.40	6.36	5.28	6.14	6.15	0.1
S (wt %)	0.76	0.63	0.50	0.67	0.57	0.27	<0.1
O* (wt %)	8.59	7.91	7.54	6.84	10.02	7.18	9.4
Water content (wt %)	2.71	1.98	1.51	1.93	1.65	2.79	<0.1
TAN	25.27	13.18	11.35	18.96	16.53	15.02	2
Heating value (MJ/kg)	37.22	35.77	30.56	37.21	35.81	36.18	39.3

* Calculated by the difference.
** Hossain et al.[64]

Except for the 500 °C in the reactor and 600 °C in the reformer condition, the oxygen values are lower than for biodiesel. This is beneficial as high oxygen contents lead to undesirable effects such as oil instability, poor combustion, and ageing effects; the lower value also reduces the amount of de-oxygenation required for bio-oil upgrading [12]. The operating conditions with the lowest reforming temperature of 500 °C produced better HHVs. The highest values of 37.22 MJ/kg and 37.21 MJ/kg were produced at reactor temperatures of 400 °C and 500 °C, respectively. These values are slightly lower than the 39.0 MJ/kg reported for the organic fraction of municipal solid waste by Kirby et al. [13]. At the 400 °C reactor temperature, there is an inverse relation between the reformer temperature and the HHV; however, this relation is not present at the 500 °C reactor temperature. The total acid number (TAN) also shows a decreasing trend with increasing reformer

temperature, which is caused by the catalytic cracking of the organic acids that takes place during the post-reforming process [63]. Lower TAN values are desired when considering the use of bio-oil as a source of engine fuels, as the high concentration of acid components leads to corrosion issues in the engine components. The lowest TAN value of 11.35 is much higher than the minimum requirement for biodiesel and higher than the 4.9 and 2.9 values reported for digestate and MSW by Neumann et al. [38] and Ouadi et al. [12], respectively.

Figure 12 shows the effect of reactor and reformer temperatures in the bio-oil dynamic viscosity at temperatures of 20 °C and 40 °C as well as the density range of the bio-oil and the aqueous phase at 20°C. With the exception of the condition at a reactor temperature of 500 °C and a reformer temperature of 600 °C, the viscosity of the bio-oil exhibits a decreasing trend as both the reactor and reformer temperatures increase. Bio-oil with the lowest dynamic viscosity of 23.92 cP at 20 °C and 10.79 cP at 40 °C was produced at 500 °C in the reactor and 650 °C in the reformer condition. At this condition, the calculated kinematic viscosity is 10.18 cSt at 40 °C, which is higher than the 6.5 cSt reported by Ouadi et al. [12] for the oil produced using MSW as feedstock. It is worth mentioning that ASTM D7544 [65] established a limit of 125 cSt for pyrolysis bio-oils; the produced bio-oil is well below the limit.

Bio-oil density, on the other hand, increases with reactor and reformer temperature, and the effect of the reformer temperature is more noticeable on density. The lowest density of 989.6 kg/m^3 was obtained at 400 °C in the reactor and 500 °C in the reformer and the highest, 1060.38 kg/m^3, at 500 °C in the reactor and 650 °C in the reformer. The bio-oil densities are slightly lower than the values considered acceptable for pyrolysis liquid Biofuels as per ASTM D7544 [65] (between 1100 kg/m^3 and 1300 kg/m^3). Compared with the aqueous phase density, bio-oil is the lighter phase at all the

process temperatures. The water content in bio-oil fluctuated between 1.51 % and 2.73 % for the different process temperatures.
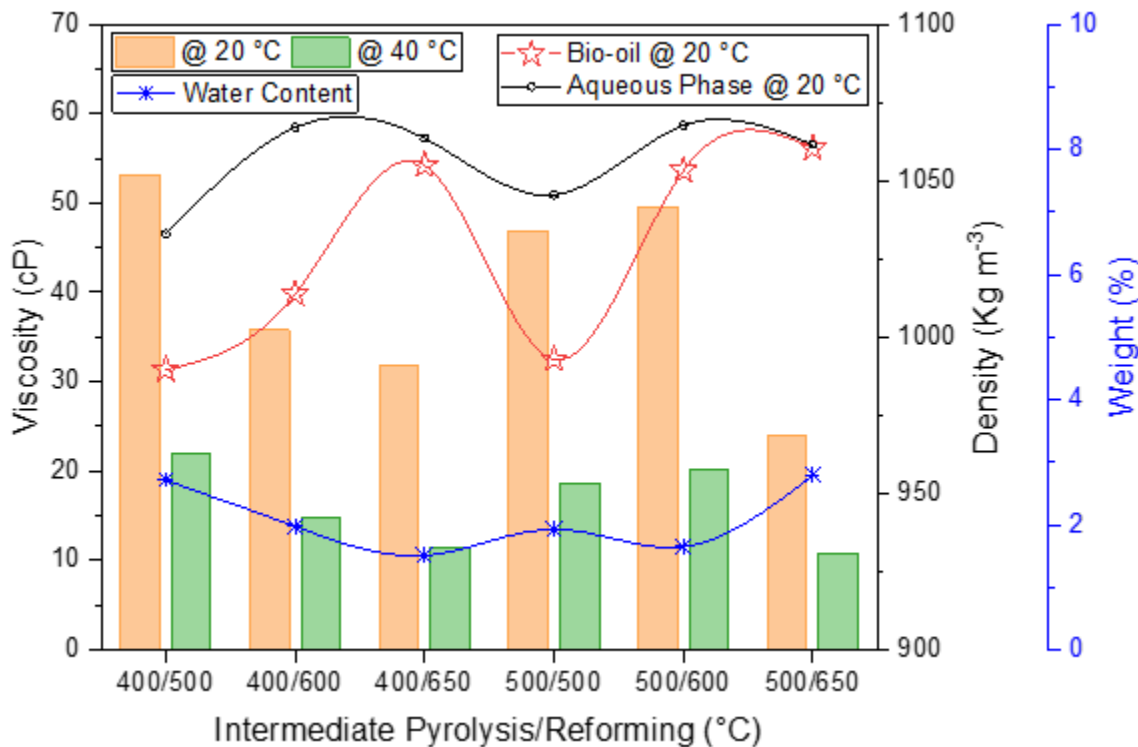
Figure 12: Viscosity of bio-oil and density of the aqueous phase and bio-oil.

The lowest aqueous phase pH of 9.17 was obtained at 400 °C in the reactor and 600 °C in the reformer, and the highest pH of 9.47 was produced at 500 °C in the reactor and 500 °C in the reformer. No clear relation between the process temperatures and the aqueous phase pH could be observed.

The compounds identified with the GC-MS were grouped into functional groups and are presented in **Table 10**. From the results, several trends are observed. The aromatic compounds include polycyclic aromatic hydrocarbons (PAHs) and monocyclic aromatic hydrocarbons (MAHs). The total amount of aromatic compounds (MAHs + PAHs) increase with higher reforming

temperatures. In contrast, alkane, alkene, and acid concentrations decrease with higher reforming temperatures. Oxygen compounds, phenols, and alcohols also decrease with higher reactor and reformer temperatures. The nitrogen compounds concentration increases with reactor temperature; however, the higher concentrations occurred at a reformer temperature of 600 °C at both reactor temperatures. Because of the wide range of compounds identified, those that did not fit into any reported functional groups were accounted for in the "unidentified" category. Dhakal's study [9] on TCR bio-oil produced from wheat straw also shows an increase in PAHs and a decrease in phenols and alcohols [48]. However, in his work, the oxygen compounds concentration increased with reactor temperature.

Given the high heterogeneity in the composition of the SSO feedstock, it is not easy to correlate the origin of the different compounds. Huang et al. [35] showed that the pyrolysis of a mix of PVC with cellulose produces bio-oil with a high concentration of PAHs [66]. They observed that the PAH concentration increased with process temperature and found a direct influence of the presence of plastics in the production of PAHs. Their findings cannot be directly associated with SSO pellets as they have a low concentration of plastics; however, they might explain the increasing trend of PAHs with increasing reforming temperature.

Table 10: GC-MS analysis of Bio-oil produced at different process temperatures. (T Reactor °C / T Reformer °C)

Compound	400/500	400/600	400/650	500/500	500/600	500/650
MAH (%)	17.4	11.9	20.1	16.2	12.2	21.3
PAH (%)	14.8	25.7	46.3	8.5	33.3	41.1
Total Aromatics (%)	**32.2**	**37.6**	**66.4**	**24.8**	**45.5**	**62.4**
Alkane (%)	4.9	2.3	1.1	8.0	2.8	0.0
Alkene (%)	8.8	1.2	0.2	13.9	0.0	1.0
Alkyne (%)	0.5	0.0	0.0	0.0	0.0	0.8
O-compound (%)	5.9	4.2	2.4	4.9	4.1	1.4
N-compound (%)	9.8	28.1	14.5	9.8	28.3	20.9

Compound	400/500	400/600	400/650	500/500	500/600	500/650
Phenols & alcohols (%)	23.8	10.0	8.3	13.3	8.3	6.4
Acids (%)	8.6	7.7	5.1	7.1	1.5	0.0
Esters (%)	0.7	0.0	0.6	0.0	0.0	0.0
Unidentified (%)	4.8	8.5	1.3	18.2	9.6	7.2

3.3.5 Energy conversion efficiency

The total energy content of the products was calculated using the product yields and identified heating values of syngas, bio-oil, and biochar. These values were compared with the total energy content of the feedstock to assess the energy conversion efficiency. The results are presented in **Figure 13**.

There is a direct relation between energy conversion efficiency and reformer temperature. Accordingly, the highest efficiency of 92.37 % occurred at 500 °C in the reactor and 650 °C in the reformer, and the lowest value of 68.64 % occurred at the lowest reactor and reformer temperatures. Syngas has a significant effect on energy conversion, as both its yield and HHV substantially increase at the higher reactor and reforming temperatures. At the more efficient condition, syngas represents 63.8 % of the total converted energy.
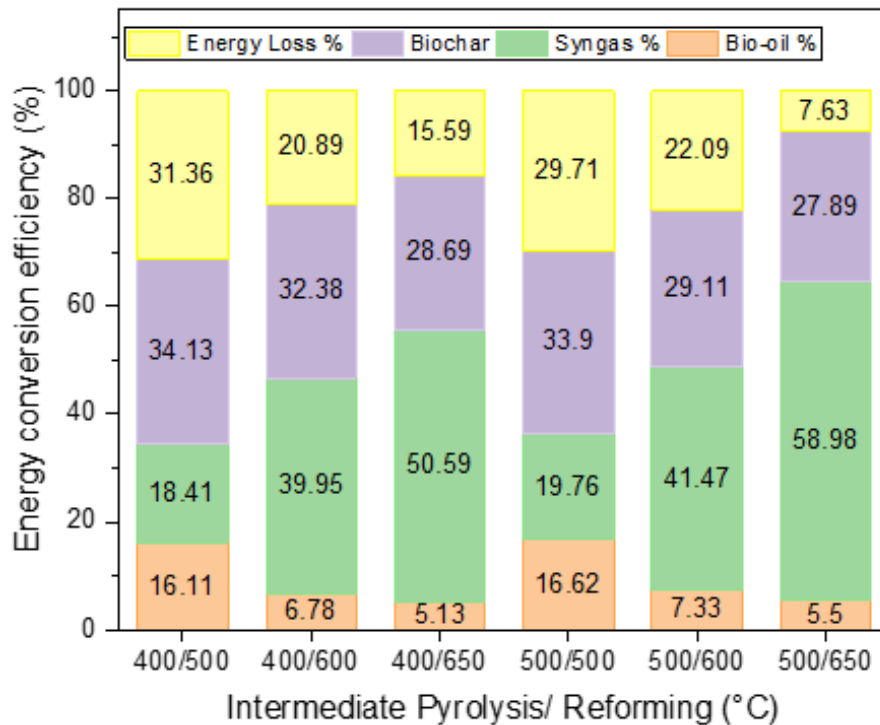
Figure 13: Energy conversion efficiency at different process temperatures.

3.4 Conclusions

Pyrolysis and gas reforming of SSO pellets were successful through the thermo-catalytic reforming (TCR) process. Up to 86.7 % of the feedstock weight could be converted to valuable products containing 92.4 % of the energy from the SSO feedstock. Based on the results, TCR technology can be considered a feasible waste-to-energy conversion pathway for SSO.

Lower process temperatures generated bio-oil with higher yields and energy contents. In contrast, higher process temperatures produced considerably less oil, with slightly lower energy content but improved quality, that is, higher density, lower viscosity, lower total acid number, and lower oxygen content, which can lead to reduced upgrading requirements.

At higher process temperatures, 42.8 % of the total feedstock mass was converted to syngas with the optimal composition. The syngas consisted of 36.4 % hydrogen, 11.1 % methane, 27.3 % carbon monoxide, and 9.6 % other non-condensable hydrocarbons and a maximum HHV of 19.13 MJ/kg. Consequently, the production of syngas plays a crucial role in the overall performance of TCR applied to SSO pellets.

The aqueous phase, with an elevated pH of 9.1-9.5, might represent up to 18.9 % of the total mass of products; thus, suitable water treatment and disposal practices must be considered for the successful implementation of TCR technology.

Depending on process temperatures, the HHV of the biochar ranges from 9.2 MJ/kg to 10.5 MJ/kg and the ash content between 64.9% and 70.9%. The developed information could help in future research on the implementation of the TCR technology for production of fuels from MSW.. Further research is required to fully characterize the biochar and explore the most suitable application for it, whether that be soil remediation, combustion, or carbon capture.

Chapter 4: Conclusions and Recommendations.

4.1 Conclusions

This work assesses the potential for thermochemical conversion through the thermo-catalytic reforming technology of fractions of municipal solid waste produced in a colder climate. As an initial step in the waste stream processing, the pelletization of digestate, source-separated organics, and refuse-derived fuels was investigated. Both digestate and SSO required an initial drying to remove their high moisture content, and RDF was delivered by the production facility at a semi-dry condition.

Table 11: Pelletization summary

	RDF	SSO
HHV (MJ/kg)	21.5	19.5 W/ 13.9 S-S
Grinding SEC (KJ/kg)	848	250
Pelletization SEC (KJ/kg)	2218	300
Bulk Density (kg/m^3)	594	683
Particle Density (kg/m^3)	996	1198
Durability (%)	98	97
Ash content (%)	9.8	13.5 W/ 34.7 S-S

SSO and RDF were successfully pelletized, but not digestate. **Table 11** present the main characteristics of the pelletization for both SSO and RDF at the optimum screen size – moisture content combinations. The effect of grinding screen size was studied, and it revealed that controlling the particle size is effective for RDF. However, for SSO, the effectiveness of the grinding screen is lower. Subsequently, the effect of particle size and moisture content on pelletization was studied. Pellets with a bulk density of up to 594 kg/m^3 for RDF and 730 kg/m^3

for SSO were produced. The maximum durability of pellets was 98.2 % for RDF and 97.4 % for SSO. The combined specific energy consumption of the grinding and pelletization was as low as 2281.15 kJ/kg for RDF pellets and 489.49 kJ/kg for SSO pellets. The HHV of the produced pellets was 21.5 MJ/kg for the RDF with 9.8 % ash content. A seasonal variation was observed in the SSO pellets. During the spring/summer seasons, the pellets exhibited a lower HHV of 13.9 MJ/kg and a higher ash content of 34.7 %. In contrast, the pellets produced during the winter had a higher HHV of 19.5 MJ/kg and lower ash content of 13.51 %.

The SSO pellets were used as feedstock for thermo-catalytic reforming. Two pyrolysis reactor temperatures (400 °C and 500 °C) and three post-reformer temperatures (500 °C, 600 °C, and 650 °C) were used to understand the effects of process temperatures on the products. **Figure 14** shows how the distribution of product yield is influenced by the process temperatures and their effect on the products energy contents. The highest process temperatures produced the highest syngas yield of 42.8 %. In the syngas, hydrogen ranged from 29 % to 36.4 %, methane from 8.8 % to 11 %, carbon monoxide from 6.9 % to 15.6 %, the heavier hydrocarbons from 9.6 % to 15.2 %; and carbon dioxide from 27.3 % to 38.3%. The syngas HHV ranged from 8.49 MJ/kg to 19.13 MJ/kg.

Low process temperatures (500 °C in both the reactor and the reformer) produced the highest bio-oil yield of 6.2 % with the highest HHV of 37.2 MJ/kg. In contrast, higher temperatures resulted in lower yields of 2.1 % but improved quality, with viscosity values as low as 10.79 cP at 40 °C, an oxygen content of 7.2 %, and a total acid number of 11.35. The highest density of 1060.38 kg/m^3 was achieved at higher process temperatures. Bio-oil produced at higher temperatures exhibited an increased concentration of aromatic hydrocarbons, reaching up to 66.4 %. At lower temperatures, the proportion of aromatics fell to as low as 24.8 %, while the content of phenols and alcohols increased to up to 23.8 %. The HHV of the biochar ranged from 9.2 MJ/kg to 10.5

MJ/kg and its ash content from 64.9 % and 70.9 %. The energy conversion efficiency was optimal at the higher process temperatures. Up to 86.7 % of the feedstock weight could be converted into bio-oil, biochar, and syngas with 92.4 % of the energy available in the SSO feedstock.
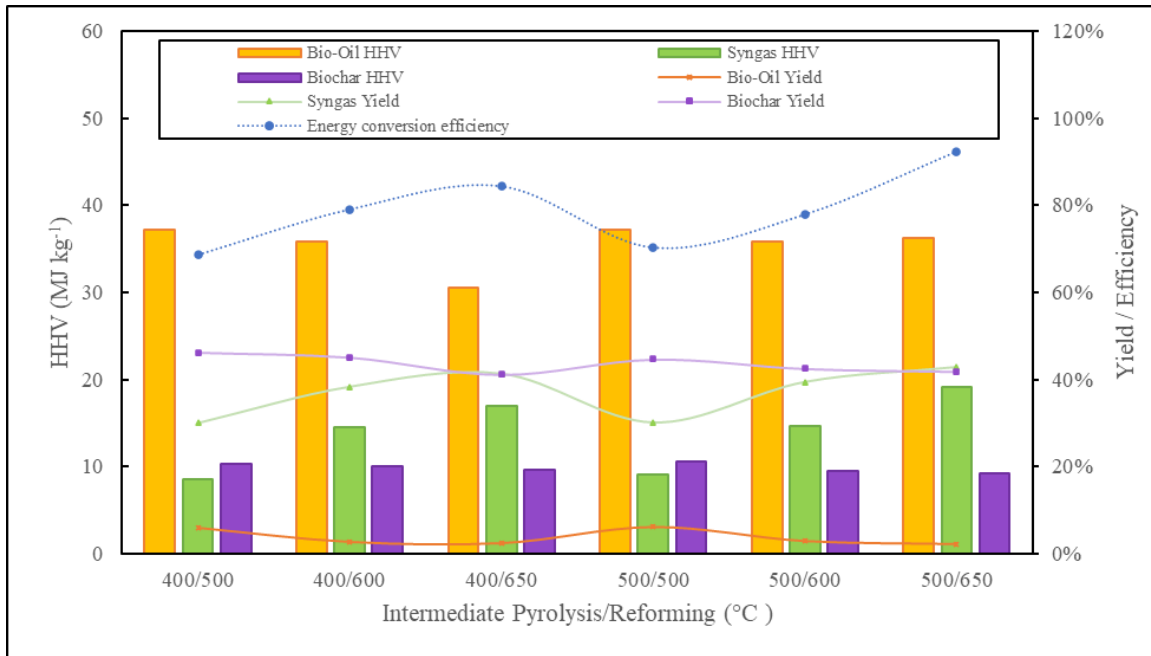
Figure 14: TCR Results summary.

Based on the results, feedstock densification by pelletization linked with thermo-catalytic reforming can be considered a feasible waste-to-energy conversion pathway for SSO. Also, the suitability of RDF for pelletization and its higher energy content suggest a potential to apply the same conversion pathway.

4.2 Recommendations

Based on the findings from the present work, the recommendations for future work are:

- A pelletization scale-up study on SSO and RDF that incorporates the drying energy requirements and assesses the use of the industrial-scale equipment available at the EWMC.

- An investigation of the seasonal effect on SSO composition and energy content as well as thermo-catalytic reforming of SSO pellets produced during the winter, given their lower ash and higher energy content.

- The thermo-catalytic reforming of RDF into biofuels and an exploration of alternatives to address the plastic content restriction in the TCR feedstock, which might include mixing RDF with SSO in proportions that allow safe operation of the TCR.

- A techno-economic analysis and a life cycle analysis of the thermo-catalytic reforming of municipal solid waste in colder climate should be carried out. The study should consider the known characteristics and product yields obtained for SSO.

- Future study should also include estimating the required upgrading processes for product commercialization and incorporation process requirements such as transport and drying, among others.

References

[1]   UN Framework Convention on Climate Change (UNFCCC). The
        Paris Agreement n.d. https://unfccc.int/process-and-meetings/the-
        paris-agreement/the-paris-agreement (accessed August 29, 2022).

[2]   Global Alliance for Incinerator Alternatives. Zero-Waste-to-Zero-
        Emissions 2022.

[3]   Climate Watch. Historical GHG Emissions n.d.
        https://www.climatewatchdata.org/ghg-
        emissions?breakBy=sector&end_year=2019&sectors=waste&source=
        Climate%20Watch&start_year=1990 (accessed June 2, 2023).

[4]   Environment and Climate Change Canada, Government of Canada.
        Canada's mid-century, long-term low-greenhouse gas emission
        development strategy. 2016. https://unfccc.int/files/focus/long-
        term_strategies/application/pdf/canadas_mid-century_long-
        term_strategy.pdf (accessed July 24, 2023).

[5]   Environment and Climate Change Canada. Solid waste diversion and
        disposal n.d. https://www.canada.ca/en/environment-climate-
        change/services/environmental-indicators/solid-waste-diversion-
        disposal.html#wb-cont (accessed August 29, 2022).

[6]   Shukla S, Khan R. Sustainable waste management approach: A
        paradigm shift towards zero waste into landfills. Advanced Organic
        Waste Management: Sustainable Practices and Approaches 2022:381–
        95. https://doi.org/10.1016/B978-0-323-85792-5.00006-X.

[7]   Marulanda VA, Gutierrez CDB, Alzate CAC. Thermochemical,
        biological, biochemical, and hybrid conversion methods of bio-
        derived molecules into renewable fuels. Advanced Bioprocessing for
        Alternative Fuels, Biobased Chemicals, and Bioproducts:

Technologies and Approaches for Scale-Up and Commercialization, Elsevier; 2019, p. 59–81. https://doi.org/10.1016/B978-0-12-817941-3.00004-8.

[8]   Sakthivel R, Harshini GV, Vardhan MS, Vinod A, Gomathi K. Biomass energy conversion through pyrolysis: A ray of hope for the current energy crisis. Green Energy Systems, Elsevier; 2023, p. 37–68. https://doi.org/10.1016/b978-0-323-95108-1.00006-9.

[9]   Hornung A. Intermediate pyrolysis of biomass. Biomass Combustion Science, Technology and Engineering, Elsevier Inc.; 2013, p. 172–86. https://doi.org/10.1533/9780857097439.2.172.

[10]   Binder S, Jakuttis M, Apfelbacher A, Hornung A. Anlage und Verfahren zur thermokatalytischen Behandlung von Material und damit hergestelltes Pyrolyseöl. 102014105340, 2015.

[11]   Neumann J, Meyer J, Ouadi M, Apfelbacher A, Binder S, Hornung A. The conversion of anaerobic digestion waste into biofuels via a novel Thermo-Catalytic Reforming process. Waste Management 2016;47:141–8. https://doi.org/10.1016/j.wasman.2015.07.001.

[12]   Ouadi M, Jaeger N, Greenhalf C, Santos J, Conti R, Hornung A. Thermo-Catalytic Reforming of municipal solid waste. Waste Management 2017;68:198–206. https://doi.org/10.1016/j.wasman.2017.06.044.

[13]   Kirby ME, Hornung A, Ouadi M, Theodorou MK. The role of thermo-catalytic reforming for energy recovery from food and drink supply chain wastes. Energy Procedia, vol. 123, Elsevier Ltd; 2017, p. 15–21. https://doi.org/10.1016/j.egypro.2017.07.279.

[14]   Chavando JAM, Silva VB, Tarelho LAC, Cardoso JS, Eusébio D. Snapshot review of refuse-derived fuels. Util Policy 2022;74. https://doi.org/10.1016/j.jup.2021.101316.

[15]   City of Edmonton. The future of Waste. n.d.

[16]   Stringfellow A, Powrie W, Tejada WC, Whatmore S, Gilbert A,
       Manser R, et al. Mechanical heat treatment of municipal solid waste.
       Proceedings of Institution of Civil Engineers: Waste and Resource
       Management, vol. 164, 2011, p. 179–90.
       https://doi.org/10.1680/warm.2011.164.3.179.

[17]   Pradhan P, Mahajani SM, Arora A. Production and utilization of fuel
       pellets from biomass: A review. Fuel Processing Technology
       2018;181:215–32. https://doi.org/10.1016/j.fuproc.2018.09.021.

[18]   Agar DA, Rudolfsson M, Kalén G, Campargue M, Da Silva Perez D,
       Larsson SH. A systematic study of ring-die pellet production from
       forest and agricultural biomass. Fuel Processing Technology
       2018;180:47–55. https://doi.org/10.1016/j.fuproc.2018.08.006.

[19]   Kratzeisen M, Starcevic N, Martinov M, Maurer C, Müller J.
       Applicability of biogas digestate as solid fuel. Fuel 2010;89:2544–8.
       https://doi.org/10.1016/j.fuel.2010.02.008.

[20]   Czekała W, Bartnikowska S, Dach J, Janczak D, Smurzyńska A,
       Kozłowski K, et al. The energy value and economic efficiency of solid
       biofuels produced from digestate and sawdust. Energy
       2018;159:1118–22. https://doi.org/10.1016/j.energy.2018.06.090.

[21]   Cathcart A, Smyth BM, Lyons G, Murray ST, Rooney D, Johnston
       CR. An economic analysis of anaerobic digestate fuel pellet
       production: can digestate fuel pellets add value to existing operations?
       Clean Eng Technol 2021;3.
       https://doi.org/10.1016/j.clet.2021.100098.

[22]   Du Y, Ju T, Meng Y, Lan T, Han S, Jiang J. A review on municipal
       solid waste pyrolysis of different composition for gas production. Fuel

Processing Technology 2021;224.
https://doi.org/10.1016/j.fuproc.2021.107026.

[23] Rezaei H, Yazdanpanah F, Lim CJ, Sokhansanj S. Pelletization
properties of refuse-derived fuel - Effects of particle size and moisture
content. Fuel Processing Technology 2020;205.
https://doi.org/10.1016/j.fuproc.2020.106437.

[24] García R, González-Vázquez MP, Rubiera F, Pevida C, Gil M v. Co-
pelletization of pine sawdust and refused derived fuel (RDF) to high-
quality waste-derived pellets. J Clean Prod 2021;328.
https://doi.org/10.1016/j.jclepro.2021.129635.

[25] Jewiarz M, Mudryk K, Wróbel M, Fraczek J, Dziedzic K. Parameters
affecting RDF-based pellet quality. Energies (Basel) 2020;13.
https://doi.org/10.3390/en13040910.

[26] Moreira BR de A, Cruz VH, Pérez JF, Viana R da S. Production of
pellets for combustion and physisorption of CO2 from hydrothermal
carbonization of food waste – Part I: High-performance solid biofuels.
J Clean Prod 2021;319. https://doi.org/10.1016/j.jclepro.2021.128695.

[27] Sharma HB, Dubey BK. Co-hydrothermal carbonization of food waste
with yard waste for solid biofuel production: Hydrochar
characterization and its pelletization. Waste Management
2020;118:521–33. https://doi.org/10.1016/j.wasman.2020.09.009.

[28] Wang T, Zhai Y, Li H, Zhu Y, Li S, Peng C, et al. Co-hydrothermal
carbonization of food waste-woody biomass blend towards biofuel
pellets production. Bioresour Technol 2018;267:371–7.
https://doi.org/10.1016/j.biortech.2018.07.059.

[29] Wang T, Wang Z, Zhai Y, Li S, Liu X, Wang B, et al. Effect of
molasses binder on the pelletization of food waste hydrochar for

enhanced biofuel pellets production. Sustain Chem Pharm 2019;14. https://doi.org/10.1016/j.scp.2019.100183.

[30]   Chew KW, Chia SR, Yap YJ, Ling TC, Tao Y, Show PL. Densification of food waste compost: Effects of moisture content and dairy powder waste additives on pellet quality. Process Safety and Environmental Protection 2018;116:780–6. https://doi.org/10.1016/j.psep.2018.03.016.

[31]   BIOFerm. FERMITIGO Dry Fermentation Case Study 2023. https://www.biofermenergy.com/wp-content/uploads/2022/08/MA_R016-Oshkosh-Case-Study-FERMITIGO.pdf (accessed July 19, 2023).

[32]   ASTM International. ASTM D7582 Standard Test Methods for Proximate Analysis of Coal and Coke by Macro Thermogravimetric Analysis. 2016. https://doi.org/10.1520/D7582-10E01.

[33]   ASTM International. ASTM E778 - Standard Test Methods for Nitrogen in Refuse-Derived Fuel Analysis Samples. 2021. https://doi.org/DOI:10.1520/E0778-15R21.2.

[34]   ASTM International. ASTM E775-15(2021) Standard Test Methods for Total Sulfur in the Analysis Sample of Refuse-Derived Fuel. 2021. https://doi.org/10.1520/E0775-15R21.

[35]   Hindrichsen IK, Kreuzer M, Madsen J, Bach Knudsen KE. Fiber and lignin analysis in concentrate, forage, and feces: Detergent versus enzymatic-chemical method. J Dairy Sci 2006;89:2168–76. https://doi.org/10.3168/jds.S0022-0302(06)72287-1.

[36]   American Society of Agricultural and Biological Engineers. STANDARD ANSI/ASAE S319.3 FEB03 Method of Determining and Expressing Fineness of Feed Materials by Sieving. 2008.

[37] Neumann J, Meyer J, Ouadi M, Apfelbacher A, Binder S, Hornung A. The conversion of anaerobic digestion waste into biofuels via a novel Thermo-Catalytic Reforming process. Waste Management 2016;47:141–8. https://doi.org/10.1016/j.wasman.2015.07.001.

[38] Neumann J, Binder S, Apfelbacher A, Gasson JR, Ramírez García P, Hornung A. Production and characterization of a new quality pyrolysis oil, char and syngas from digestate - Introducing the thermo-catalytic reforming process. J Anal Appl Pyrolysis 2015;113:137–42. https://doi.org/10.1016/j.jaap.2014.11.022.

[39] International Organization for Standardization. ISO 9276 - 1 Representation of results of particle size analysis - Part 1: Graphical representation. 2004.

[40] Pradhan P, Arora A, Mahajani SM. Pilot scale evaluation of fuel pellets production from garden waste biomass. Energy for Sustainable Development 2018;43:1–14. https://doi.org/10.1016/j.esd.2017.11.005.

[41] Samuelsson R, Larsson SH, Thyrel M, Lestander TA. Moisture content and storage time influence the binding mechanisms in biofuel wood pellets. Appl Energy 2012;99:109–15. https://doi.org/10.1016/J.APENERGY.2012.05.004.

[42] International Organization for Standardization. ISO 17225-6 Solid biofuels-Fuel specifications and classes-Part 6: Graded non-woody pellets. 2021.

[43] International Energy Agency, IEA Publications. Canada 2022 - Energy Policy Review. 2022.

[44] Marulanda VA, Gutierrez CDB, Alzate CAC. Thermochemical, biological, biochemical, and hybrid conversion methods of bio-derived molecules into renewable fuels. Advanced Bioprocessing for

Alternative Fuels, Biobased Chemicals, and Bioproducts:
Technologies and Approaches for Scale-Up and Commercialization,
Elsevier; 2019, p. 59–81. https://doi.org/10.1016/B978-0-12-817941-
3.00004-8.

[45]   Sakthivel R, Harshini GV, Vardhan MS, Vinod A, Gomathi K.
Biomass energy conversion through pyrolysis: A ray of hope for the
current energy crisis. Green Energy Systems, Elsevier; 2023, p. 37–
68. https://doi.org/10.1016/b978-0-323-95108-1.00006-9.

[46]   Kurian V, Gill M, Dhakal B, Kumar A. Recent trends in the pyrolysis
and gasification of lignocellulosic biomass. Biofuels and Bioenergy:
A Techno-Economic Approach, Elsevier; 2022, p. 511–52.
https://doi.org/10.1016/B978-0-323-90040-9.00028-X.

[47]   Gill M, Kurian V, Kumar A, Stenzel F, Hornung A, Gupta R. Thermo-
catalytic reforming of alberta-based biomass feedstock to produce
biofuels. Biomass Bioenergy 2021;152.
https://doi.org/10.1016/j.biombioe.2021.106203.

[48]   Dhakal B. Intermediate pyrolysis of wheat straw and softwood pellets.
MSc Thesis. University of Alberta, 2021.

[49]   Kick C, Uchaikina A, Apfelbacher A, Daschner R, Helmreich B,
Hornung A. Aqueous phase of thermo-catalytic reforming of sewage
sludge – quantity, quality, and its electrooxidative treatment by a
boron-doped diamond electrode. Sep Purif Technol 2022;286.
https://doi.org/10.1016/j.seppur.2021.120392.

[50]   Hornung U, Schneider D, Hornung A, Tumiatti V, Seifert H.
Sequential pyrolysis and catalytic low temperature reforming of wheat
straw. J Anal Appl Pyrolysis 2009;85:145–50.
https://doi.org/10.1016/j.jaap.2008.11.006.

[51] Hasan MM, Rasul MG, Khan MMK, Ashwath N, Jahirul MI. Energy recovery from municipal solid waste using pyrolysis technology: A review on current status and developments. Renewable and Sustainable Energy Reviews 2021;145. https://doi.org/10.1016/j.rser.2021.111073.

[52] Hornung A, Jahangiri H, Ouadi M, Kick C, Deinert L, Meyer B, et al. Thermo-Catalytic Reforming (TCR)–An important link between waste management and renewable fuels as part of the energy transition. Applications in Energy and Combustion Science 2022;12. https://doi.org/10.1016/j.jaecs.2022.100088.

[53] ASTM International. ASTM E777 REV A - Standard Test Method for Carbon and Hydrogen in the Analysis Sample of Refuse- Derived Fuel 2017.

[54] Krotz L. Elemental Analysis: high productivity of Thermo Scientific FlashSmart N/Protein-CHNS Analyzer with the MultiValve Control (MVC) Module. n.d.

[55] IKA ®-WERKE. IKA Calorimeter System C 2000 basic / control. n.d.

[56] ASTM International. ASTM D 4377-00 Standard Test Method for Water in Crude Oils by Potentiometric Karl Fischer Titration. n.d.

[57] Carbognani L, Roa-Fuentes LC, Diaz L, Berezinski J, Carbognani-Arambarri L, Pereira-Almao P. Reliable determination of water contents of bitumen and vacuum residua via coulometric Karl Fischer titration using tetrahydrofuran. Pet Sci Technol 2014;32:602–9. https://doi.org/10.1080/10916466.2011.599194.

[58] ASTM International. ASTM D664 - 04 Standard Test Method for Acid Number of Petroleum Products by Potentiometric Titration 1. n.d.

[59] DIN - Deutsches Institut für Normung e. V. DIN 53019-1 -
Viscometry - Measurement of viscosities and flow curves by means of
rotational viscometers - Part 1: Principles and geometry of measuring
system 2008.

[60] ASTM International. ASTM D4052 - Standard Test Method for
Density and Relative Density of Liquids by Digital Density Meter 1.
n.d.

[61] Waldheim L, Nilsson T. Heating value of gases from biomass
gasification. Report prepared for: IEA Bioenergy Agreement, Task
20-Thermal Gasification of Biomass. 2001.

[62] Sheng C, Azevedo JLT. Estimating the higher heating value of
biomass fuels from basic analysis data. Biomass Bioenergy
2005;28:499–507. https://doi.org/10.1016/j.biombioe.2004.11.008.

[63] Neumann J, Meyer J, Ouadi M, Apfelbacher A, Binder S, Hornung A.
The conversion of anaerobic digestion waste into biofuels via a novel
Thermo-Catalytic Reforming process. Waste Management
2016;47:141–8. https://doi.org/10.1016/j.wasman.2015.07.001.

[64] Hossain AK, Ouadi M, Siddiqui SU, Yang Y, Brammer J, Hornung A,
et al. Experimental investigation of performance, emission and
combustion characteristics of an indirect injection multi-cylinder CI
engine fuelled by blends of de-inking sludge pyrolysis oil with
biodiesel. Fuel 2013;105:135–42.
https://doi.org/10.1016/j.fuel.2012.05.007.

[65] ASTM International. ASTM D7544 − 12 Standard Specification for
Pyrolysis Liquid Biofuel 1 n.d. https://doi.org/10.1520/D7544-12.

[66] Huang Q, Tang Y, Lu S, Wu X, Chi Y, Yan J. Characterization of Tar
Derived from Principle Components of Municipal Solid Waste.

Energy and Fuels 2015;29:7266–74.

https://doi.org/10.1021/acs.energyfuels.5b01152.